



# On the transient planar contact problem in the presence of dry friction and slip

B. Gurrutxaga-Lerma

School of Metallurgy and Materials, University of Birmingham, B15 2SE Edgbaston, Birmingham, UK

## ARTICLE INFO

### Article history:

Received 26 November 2019

Revised 17 February 2020

Accepted 18 February 2020

Available online 21 February 2020

### Keywords:

Elastodynamic

Contact

Plane strain

Stick

Slip

Friction

## ABSTRACT

This article models a plane strain dynamic contact problem for an infinite elastic body. Contact is established for  $x > 0$  under the action of a time-dependent remote compressive load, and the system is subjected to a time-dependent remote tangential load. The two faces of the contact interface can slide relative to one other to accommodate mismatches between the shear stresses and the existing Coulomb friction. This is shown to be a cause of interfacial waves of slip, which this article models by deriving the general expression for the corrective traction due to an arbitrary slip distribution. This is achieved using a variant of the Wiener-Hopf technique. Combined with existing closed-form expressions for the interfacial tractions due to compressive and shear loads, this enables the formulation of the elastodynamic extension to the stick-and-slip problem of the Cattaneo-Mindlin type. Exploiting self-similarity a simple numerical algorithm is detailed for solving the resulting Volterra integral equations of the first kind. The solution is shown to display a number of features entirely missed in static problems: slip waves are shown to exist irrespective of the magnitude of the applied loads and the friction coefficient; a regime of reverse and forward slip is also shown to exist for low friction coefficients, brought about by the interfacial Rayleigh waves. The practical implications of these solutions are discussed.

© 2020 Elsevier Ltd. All rights reserved.

## 1. Introduction

This article concerns the fundamental solution to the planar elastodynamic contact problem between two elastically similar bodies subject to friction and slip. By elastodynamic contact, we mean contact where the time-dependencies involved in the transmission of loads and displacements are fully accounted for. These time-dependencies are brought about by the internal inertial forces acting in any material with mass, and manifest themselves as *elastic* waves that propagate at the material's speeds of sound, i.e., over finite timescales. Because the speeds of sound in most solids typically exceed 1000 m/s (Eringen and Suhubi, 1975), 'dynamic' or 'elastodynamic' contact of this sort is relevant over short timescales or when the representative time and lengthscales are comparable to the material's speeds of sound. This may be the case when the contacting bodies endure loading *transients*, that is to say, when the loading (or the loading rate) changes quickly over short periods of time. Under such circumstances, the contact interface may be subjected to rapidly varying time-dependent loads that deviate considerably from the static, time-independent considerations that govern the classical problems of contact mechanics (see Barber, 2018; Johnson, 1987).

Owing to the inherent complexities of contact mechanics in general, and of elastodynamics in particular, the study of elastodynamic contact in the presence of friction has received considerably less attention than it ought to. Indeed, there exist a considerable number of practical applications where loading transients affect contacting interfaces. Such situations are found in the bearings of rotating machinery (e.g., gas turbine shaft bearings (Khonsari and Booser, 2008; Torkhani et al., 2012; Hirani et al., 1999; Schwing-shackl et al., 2012) or wind turbine shafts (Morren et al., 2006; Kotzalas and Doll, 2010)) and small devices (Palm and Murphy, 1999; Williams, 2001); in structural applications involving vibrations (Duffour and Woodhouse, 2004a; 2004b; 2007; Gaul and Lenz, 1997; Gaul and Nitsche, 2001); or in brakes, where dynamic contact is involved in frictional induced vibrations (Nack, 2000; Butlin and Woodhouse, 2009). In all these applications, the loads at the contact interface can vary quickly in time, and the conventional contact conditions that are known to dominate the steady state response (q.v. Barber, 2018; Johnson, 1987) need to be re-examined under fully time-dependent, inertial considerations.

Problems involving planar moving contact in the absence of friction have been the subject of much work in the past (Barber, 2018). A number of noteworthy solutions include Galin's study of the moving punch on a half-space (Galin, 1961), and Thompson and Robinson's (Robinson and Thompson, 1974) solu-

E-mail address: [b.gurrutxagalerna.1@bham.ac.uk](mailto:b.gurrutxagalerna.1@bham.ac.uk)

tion for the transient motion of a wedge-like uniformly moving indenter (see also Brock, 1976; Brock, 1981; Kubenko and Popov, 1988; Slepnyan and Brun, 2012), which effectively extend Hertzian contact problems to fully inertial settings (Brock, 1978; Bedding and Willis, 1973). This approach has proven particularly useful in studying the role inertial forces may play in kinetic sliding contacts under plane strain (Georgiadis and Barber, 1993; Brock, 2002), revealing the role the Rayleigh wave speed and the speeds of sound play in the possibility of trans and supersonic sliding (Slepnyan and Brun, 2012). A number of studies accounting for the effect of friction also exist. Building on the frictionless family of problems, Brock (1979, 1981, 1993) and Brock and Georgiadis (1994) and Georgiadis et al. (1995) introduced Coulombian friction to the study of uniformly driven wedge indentation problems, focusing on the effect dry friction had in the singularities arising in the interfacial tractions. Similar problems involving uniformly moving round indenters subjected to linear friction were studied by Borodich and Gomatam (1998).

Furthermore, the study of the transient response of contacting bodies with (and without) friction has a considerable corpus of work devoted to studying the instabilities affecting the contact interface under dynamic loading. Rather than seeking explicit transient solutions, these studies aim at studying the ill-posedness of the problem using stability analysis (Menq and Griffin, 1985; Berger et al., 2000; Persson, 2001; Colin, 2016). Early insights from this approach focused on frictionless studies, such as those by Achenbach and Epstein (1967), who considered planar interfaces excited by free time-harmonic waves, or by Comninou and Dundurs (1977), who studied interfacial separation along bimaterial interfaces. Subsequent studies of this sort, such as those by Renardy (1992) and Martins et al. (1995) extended the approach to account for the presence of friction, showing that large frictional coefficients favoured instabilities. Weertman (1980), in analysing through perturbative approaches the effect a traveling distribution of dislocations would have on the shear and normal interfacial tractions, found that self-sustained slip pulses were possible even in the presence of Coulombian-like friction. These pulses were linked to the Schallamach waves (Schallamach, 1971), i.e., the waves of detachment observed in the slip of rubber; similar waves of detachment have also been observed along geological interfaces (Ben-David et al., 2010; Ben-David and Fineberg, 2011; Rubinstein et al., 2004; 2007). Finally, in studying the stability of the steady state solution to the planar contact between two dissimilar materials, Adams (1995) showed the existence of the so-called *Adams instabilities*, which can lead to separation and waves of stick and slip.

This article aims to extend the existing corpus of explicit elastodynamic solutions, in an attempt to generalise the classical ‘stick-and-slip’ (Cattaneo, 1938; Mindlin, 1949) style contact problems to fully time-dependent settings. In this family of problems, a normal and a tangential load are applied over two contacting bodies. Because tangential loads can only be transmitted across the interface via frictional forces, a frictional force is required to act along the interface (Barber (2018)), usually under the assumption that Amontons’ law (cf. Amontons, 1699) holds. In order to accommodate imbalances between the normal and tangential interfacial tractions, it is possible that the interface itself be allowed to slip, i.e., undergo a shear deformation. To that end, the traditional Cattaneo-Mindlin style approach introduces a ‘corrective’ interfacial traction generated by the distribution of slip (Johnson, 1987), the description of which can be provided in a number of ways, including as a continuous distribution of straight dislocations (see for instance Hills et al., 1996; Hills and Nowell, 1994; Nowell et al., 1988). In Gurrutxaga-Lerma (2019), the author discussed how to express the interfacial shear slip of an antiplanar contact subjected to inertial loads as a distribution of Burgers vectors. In so doing, the con-

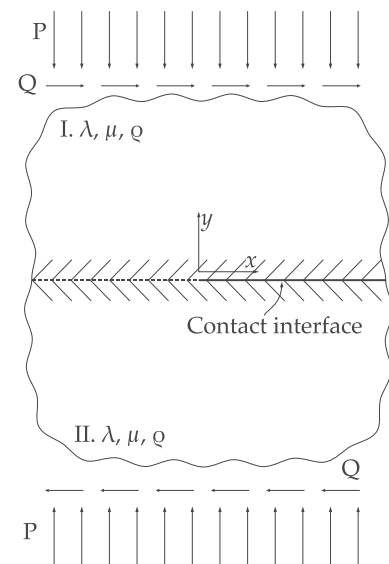


**Fig. 1.** Schematic of the contact problem under consideration. The problem consists of two elastically similar bodies, I and II, of Lamé parameter  $\lambda$ , shear modulus  $\mu$  and density  $\rho$ . The two bodies are semi-infinite half planes. Contact is established on the  $x > 0$  line as a result of the action of the remote normal load  $P$ . This entails a normal contact traction along the contact interface, and as a result a frictional force acting in the shearing direction.

tact problem was shown to resemble the classical (Cattaneo, 1938; Mindlin, 1949) problem, but owing to the time dependencies implied by the inherently transient, elastodynamic contact loads, the problem could only be solved numerically to highlight the presence of a regime of transient forward and reverse slip.

This article focuses on the non-trivial planar case, by which we mean the case when the normal and tangential loads are co-planar with the normal vector of the contact interface. Thus, this article is structured as follows. Section 2 describes the general characteristics of the elastodynamic planar contact problem, highlighting the need to describe the interfacial shear tractions due to a remote load and due to an unknown slip distribution. The interfacial normal and tangential tractions problem due to remote loading have well-known (Achenbach, 1973; Aki and Richards, 2002; Freund, 1998) solutions, which are briefly outlined in Section 3. The interfacial shear traction problem due to a slip distribution is solved in Section 4 by deriving the fundamental solution for the relevant problem. Section 5 provides the full governing equation and outlines a numerical method for its solution, which is solved in Section 6. Section 7 closes this article with its concluding remarks.

## 2. Constitutive hypotheses

We will consider the system depicted in Fig. 1, comprising of two elastically similar infinite bodies of Lamé parameter  $\lambda$ , shear modulus  $\mu$  and density  $\rho$ . The infinite body is loaded by remote normal  $P$  and shear  $Q$  loads, which will trigger compressive and shear waves at the contact interface, defined for  $x > 0$ . The part of the bodies not in touch ( $x < 0$ ) forms in effect a mode I/mode II elastodynamic crack. The two sides of the contact interface can slip relative to each other when shear stresses reach the Coulomb limiting value. In the sequel, the slip velocity will be assumed to be sufficiently small for the sliding to remain subcritical (cf. Slepnyan and Brun, 2012).

Contact is established through the mediation of the remote normal load  $P$ , and under the presence of a remote tangential load  $Q$ .

Each induce, respectively, a distributed normal traction  $p(x, t)$  and a distributed shear traction  $q(x, t)$  along the contact interface, which propagate along the interface in the form of waves. Hereafter, we shall assume that both loads are uncoupled. This means that the main role of the normal load,  $P$  is to ensure that the two interfaces remain in contact throughout. However, the normal tractions induce no slip along the contact interface and, therefore, in the absence of an external shear traction the normal load is on its own unable to induce any kind of shear traction at the interface, so that the interface would remain in conditions of perfect *stick*.

If both a normal and a shear traction are applied, the shear traction can only be transmitted across the interface via frictional forces (Barber, 2018; Johnson, 1987). These frictional forces arise in opposition to the applied shear traction and the relative motion of the interface, for otherwise friction would not be dissipative. In the following, we shall assume that the frictional forces obey Coulomb's law, which is to say, they are proportional to the normal load via a friction coefficient  $f$  (Johnson, 1987):

$$F_{\text{frict}}(x, t) = -f \text{sign}(f) p(x, t) = -f \frac{\dot{u}(x, t)}{|\dot{u}(x, t)|} p(x, t) \quad (2.1)$$

where  $f$  is the coefficient of friction, which we shall assume is constant, and  $\dot{u}(x, t)$  is the relative tangential speed of the interfacial point  $x$  at time  $t$ . Although considerations involving the potential velocity dependence of the friction coefficient itself would be pertinent in some applications (see for instance Molinari and Perfettini, 2017; Perfettini and Molinari, 2017), these would require more complex numerical approaches; hence this study focuses on the Coulombian frictional case alone.

In principle, the shear traction must be accommodated by the frictional force. This is because the role of the frictional force is to ensure the transmission of the shear traction. However, due to the specificities of the loading conditions and of the frictional forces at the interface, it is possible that the frictional force and the shear tractions arising due to the external loading not balance one another. In that case, the interface will tend to *slip* locally until the force balance is restored. Thus, we have a clear-cut distinction in the interfacial force balance at the contact interface, depending on whether the interface is a region of stick or a region of slip:

- In a stick region,  $|q(x, t)| \leq F_{\text{frict}}(x, t)$ , and  $\dot{u}(x, t) = 0$ .
- In a slip region,  $|q(x, t)| = F_{\text{frict}}(x, t)$  and  $\dot{u}(x, t) \neq 0$ .

where hereafter we will denote the (in-plane) displacement vector  $u_i(x, t)$  through its cartesian components  $u(x, t) \equiv u_x(x, t)$  and  $v(x, t) \equiv u_y(x, t)$  for the horizontal and vertical displacement components, respectively. Equally, the slip velocity  $\dot{u}_i(x, t)$  components are denoted with  $\dot{u}(x, t)$  and  $\dot{v}(x, t)$ , respectively. We seek to provide an expression for the interfacial loads at play. This is done in Sections 3 and 4. In finding  $s(x, t)$ , we shall be able to describe the way the interface slips, as well as the spatial bounds of the region of slip. We shall by default define the compressive normal load as positive.

### 3. Traction distribution due to the normal and tangential loads

The system is subjected to a remote normal load  $P$  and to a remote tangential load  $Q$ . We shall first assume that  $P$  and  $Q$  are independent from one another, and that the time dependent and spatially dependent parts can be separated, i.e., that  $P = P(x)n(t)$  and  $Q = Q(x)s(t)$ . The normal load induces a certain distribution of normal tractions  $p(x, t)$ ; the tangential load induces a certain distribution of shear tractions  $q(x, t)$ . Expressions for both such loads are available in the general literature (Freund, 1998; Broberg, 1999; Achenbach, 1973).

#### 3.1. General displacements due to point loads acting on the interface

In the interest of mirroring the development of the classical Cattaneo-Mindlin problem (see Barber, 2018; Johnson, 1987 for modern accounts), we will first state the elastodynamic displacement fields due to the action of a normal point force  $F_y$  and tangential shear force  $F_x$  on an elastic body. These displacement fields stand in direct analogy to the Flamant solutions (Barber, 2018) in elastostatics, and were originally deduced by Lamb (1904). Here, we reproduce the displacement field components acting along a flat surface. More complete versions of the Lamb solutions are collected by Eringen and Suhubi (1975, pp.614-618).

Thus, we have that Eringen and Suhubi (1975)

$$u_x(x, t) = -F_y \text{sign}(x) \left[ \frac{2b^2}{\pi\mu} U_2\left(\frac{t}{x}\right) - K\delta\left(t - \frac{|x|}{c_R}\right) \right] + F_x \frac{b^2}{\pi\mu} \frac{1}{|x|} U_1\left(\frac{t}{x}\right) \quad (3.1)$$

$$u_y(x, t) = F_y \frac{b^2}{\pi\mu} \frac{1}{|x|} V_2\left(\frac{t}{x}\right) + F_x \text{sign}(x) \left[ \frac{2b^2}{\pi\mu} V_1\left(\frac{t}{x}\right) + K\delta\left(t - \frac{|x|}{c_R}\right) \right] \quad (3.2)$$

where  $a = 1/c_l$  and  $b = 1/c_t$  are the longitudinal and transverse slownesses of sound, respectively, and  $c_l$ ,  $c_t$  and  $c_R$ , the longitudinal and transverse speeds of sound, and the Rayleigh wave speed, respectively; and where

$$U_1(u) = \begin{cases} -\frac{\sqrt{u^2-b^2}}{(b^2-2u^2)^2-4u^2\sqrt{u^2-a^2}\sqrt{u^2-b^2}} & u > b \\ \frac{4u^2(b^2-u^2)\sqrt{u^2-a^2}}{(b^2-2u^2)^4+16u^4(u^2-a^2)(b^2-u^2)} & a < u < b \\ 0 & \text{otherwise} \end{cases}$$

$$V_1(u) = \begin{cases} -\frac{|u|(2u^2-b^2)\sqrt{u^2-a^2}\sqrt{b^2-u^2}}{(b^2-2u^2)^4+16u^4(u^2-a^2)(b^2-u^2)} & a < u < b \\ 0 & \text{otherwise} \end{cases}$$

$$U_2(u) = -V_1(u)$$

$$V_2(u) = \begin{cases} -\frac{(b^2-2u^2)^2\sqrt{u^2-a^2}}{(b^2-2u^2)^4+16u^4(u^2-a^2)(b^2-u^2)} & a < u < b \\ -\frac{\sqrt{u^2-a^2}}{(b^2-2u^2)^2-4u^2\sqrt{u^2-a^2}\sqrt{u^2-b^2}} & u > b \end{cases}$$

and

$$K = b^2 \frac{2(c_R b)^2 - 1}{\mu c_R \chi_R}$$

where  $u = t/x$  and  $\chi_R$  is given in the Appendix.

For simplicity, it is useful to define planar half-space Green's function  $G_{ij}(x, t)$ , with components:

$$\begin{aligned} G_{11}(x, t) &= \frac{b^2}{\pi\mu} \frac{1}{|x|} U_1\left(\frac{t}{x}\right), \\ G_{12}(x, t) &= -\text{sign}(x) \left[ \frac{2b^2}{\pi\mu} U_2\left(\frac{t}{x}\right) - K\delta\left(t - \frac{|x|}{c_R}\right) \right] \\ G_{21}(x, t) &= \text{sign}(x) \left[ \frac{2b^2}{\pi\mu} V_1\left(\frac{t}{x}\right) + K\delta\left(t - \frac{|x|}{c_R}\right) \right], \\ G_{22}(x, t) &= \frac{b^2}{\pi\mu} \frac{1}{|x|} V_2\left(\frac{t}{x}\right) \end{aligned} \quad (3.3)$$

### 3.2. Displacement field due to a distributed load on the interface

The Lamb solutions can be employed to express the displacement fields due to general distributed loads. Let  $p(x, t) \times q(x, t)$  be a compactly supported distributed traction acting on a planar interface, with support  $\mathcal{A}(t) = \{(x, t) \in \mathbb{R}^2 : p(x, t) \neq 0\}$ , and  $p(x, t)$  the normal component,  $q(x, t)$  the tangential component. Then the following representation formula provides the displacement field acting along the interface as

$$u_x(x, t) = \int_{\mathcal{A}(t')} G_{11}(x - x', t - t') p(x', t') + G_{12}(x - x', t - t') q(x', t') dx' dt', \quad (3.4)$$

$$u_y(x, t) = \int_{\mathcal{A}(t')} G_{21}(x - x', t - t') p(x', t') + G_{22}(x - x', t - t') q(x', t') dx' dt', \quad (3.5)$$

As in the static problem, we seek to describe the contact surface via its displacement gradient,

$$\frac{\partial u_y}{\partial x} = \int_{\mathcal{A}(t')} \left[ \frac{\partial G_{21}}{\partial x}(x - x', t - t') p(x', t') + \frac{\partial G_{22}}{\partial x}(x - x', t - t') q(x', t') \right] dx' dt' \quad (3.6)$$

Unfortunately, in this case the convolution does not result in kernels as simple it does in the static case (q.v. Barber, 2018).

### 3.3. Statement of the general problem

The pressure distribution on a planar interface would set

$$\frac{\partial u_y}{\partial x} = 0 \quad (3.7)$$

Say contact begins at  $t = 0$  and is established only over the positive real line  $x > 0$ :

$$\int_0^t \int_0^\infty \left[ \frac{\partial G_{21}}{\partial x}(x - x', t - t') p(x', t') + \frac{\partial G_{22}}{\partial x}(x - x', t - t') q(x', t') \right] dx' dt' = 0 \quad (3.8)$$

We presume that the interface remains fully stuck, so that:

$$\frac{\partial u_x}{\partial t} = 0 \quad (3.9)$$

The combination of the Eqs. (3.8) and (3.9) provides a complete account of the solution to the elastodynamic solution to the fully stuck contact problem.

### 3.4. Normal loading

As stated above, here we assume that the normal and tangential tractions are fully uncoupled. Contact is established by the application of a remote normal load  $P$ . At the contact interface, this results in a normal traction distribution  $p(x, t)$  given by the normal traction acting along the crack path of a mode I quiescent crack subjected to some remote loading  $P$ . In principle, this problem could be solved by setting  $q(x, t) = 0$  and solving Eq. (3.8). Given the inherent complexity of the elastodynamic convolution kernels, it is simpler to regard this problem from the viewpoint of fracture, where it represents the sudden loading of a mode I crack with the crack tip located on  $x = 0$ , and the crack faces on  $x < 0$ . This problem is the main concern of dynamic fracture, and a full account of its solution procedure can be found for instance in Freund (1998) or Broberg (1999).

If the remote load is sudden and spatially homogeneous,  $P(x, t) = P_0 H(t)$ , Freund (1998) discussed how using the Wiener-Hopf technique that the interfacial normal traction along the path of a mode I crack (and, by extension, along our contact interface) is given by:

$$p(x, t) = P_0 - \frac{1}{\pi x} \int_{ax}^t \text{Im} \left[ \Sigma_+ \left( -\frac{\tau}{x} \right) \right] d\tau H(t - ax) \quad (3.10)$$

where  $a = 1/c_l$  is the longitudinal slowness of sound,  $b = 1/c_t$  the transverse slowness of sound, and

$$\Sigma_+(k) = \frac{P_0}{k} \left( \frac{F_+(0)}{F_+(k)} - 1 \right), \quad F_+(k) = \frac{\sqrt{a+k}}{(c+k)S_+(k)}, \quad (3.11)$$

where  $c = 1/c_R$  is the inverse of the Rayleigh wave speed  $c_R$ , and

$$\ln S_+(k) = -\frac{1}{\pi} \int_a^b \frac{1}{u+k} \arctan \left[ \frac{4u^2 \sqrt{u^2 - a^2} \sqrt{b^2 - u^2}}{(b^2 - 2u^2)^2} \right] du \quad (3.12)$$

Eq. (3.10) provides a full field, closed-form solution to the interfacial elastodynamic normal traction. It is nevertheless possible to examine the asymptotic near field, where the solution is reduced to (Freund, 1998):

$$p(x, t) \approx \frac{K_I(t)}{\sqrt{2\pi x}}, \quad K_I(t) = \frac{2P_0 \sqrt{(1-2\nu)t}}{(1-\nu)\sqrt{\pi a}} \quad (3.13)$$

The  $1/\sqrt{x}$  singularity at the edge of the contact zone is similar to the one present in the asymptotic contact problems concerning similar geometries (Dini and Hills, 2003; Hills et al., 2012).

### 3.5. Tangential loading

The tangential loading concerns the application of a remote tangential load  $Q(x, t)$ , which induces an interfacial tangential load  $q(x, t)$ . If we assume that the contact interface remains fully stuck so that  $|q(x, t)| \leq f p(x, t)$ , then the stick condition that  $\partial_t u_x(x, t) = 0$  leads to

$$\int_0^t \int_0^\infty \frac{\partial^2 G_{21}}{\partial t \partial x}(x - x', t - t') q(x', t') dx' dt' = 0$$

is satisfied. The combination of the stick condition  $\partial_t u_x(x, t) = 0$  and the remote loading is equivalent to the loading conditions found in a mode II quiescent (non-propagating) dynamic crack subject to some remote loading  $Q(x, t)$ . This problem is also agreeable to a fully closed-form solution, which may be found in Freund (1998, sec.2.6). The interfacial tangential load  $q(x, t)$  is given by:

$$q(x, t) = Q_0 - \frac{1}{\pi x} \int_{ax}^t \text{Im} \left[ T_+ \left( -\frac{\tau}{x} \right) \right] d\tau H(t - ax) \quad (3.14)$$

where in this case

$$T_+(k) = \frac{Q_0}{k} \left( \frac{G_+(0)}{G_+(k)} - 1 \right), \quad G_+(k) = \frac{\sqrt{b+k}}{(c+k)S_+(k)}, \quad (3.15)$$

where  $S_+(k)$  is given by Eq. (3.12).

As in the normal case, an asymptotic near field solution may be given, expressed in terms of a dynamic stress intensity factor  $K_{II}(t)$ :

$$q(x, t) \approx \frac{K_{II}(t)}{\sqrt{2\pi x}}, \quad K_{II}(t) = \frac{2Q_0 \sqrt{2t}}{\sqrt{(1-\nu)\pi b}} \quad (3.16)$$

Again, the asymptotic solution presents the expected  $1/\sqrt{x}$  singularity at the edge of the contact zone.



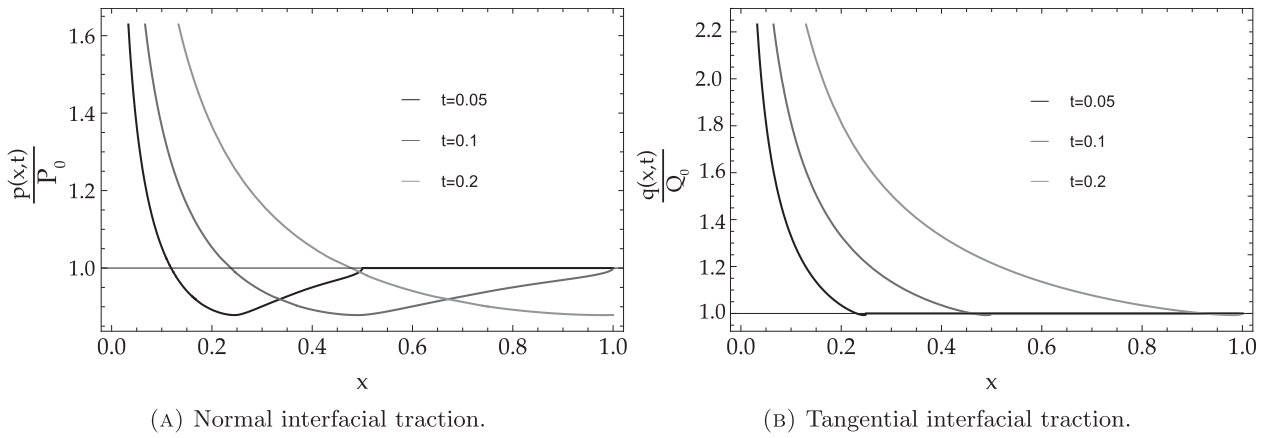


**Fig. 2.** Temporal evolution of the normal and shear tractions due to a suddenly applied remote normal and tangential suddenly applied loads.

### 3.6. Qualitative discussion of the elastodynamic contact problem

The solutions discussed in Sections 3.4 and 3.5 can be interpreted as deviations from a steady state behaviour: if the loads are changed, then the waves entailed by Eqs. (3.10) and (3.14). It is therefore possible to model the time dependencies involved in the elastodynamic contact problem by uncoupling the static behaviour from the time-dependent behaviour, and if required superposing them both. Thus, in the sequel only the time-dependencies involved in the contact problem (i.e., the integrals in Eqs. (3.10) and (3.14)) will be studied.

The asymptotic near fields of both the normal and shear tractions display a  $1/\sqrt{x}$  singularity at the origin, the magnitude of which increases over time with  $\sqrt{t}$ . However, the near fields do not propagate away from the crack tip, so they appear unsuitable for the purposes of studying the elastodynamic contact problem: both the shear and normal load would act instantaneously everywhere along the contact interface, which defeats the point of an elastodynamic treatment. The reasons for this may be found in Fig. 2a and b, which show, respectively, the time evolution of the full solution to the  $p(x, t)$  and  $q(x, t)$  loads. As can be seen, both solutions are  $1/\sqrt{x}$  singular at the origin, but the normal load  $p(x, t)$  propagates at the longitudinal speed of sound, whereas the tangential load  $q(x, t)$  propagates at the slower transverse speed of sound.

#### 3.6.1. Stick and slip

For contact to be established, it is necessary that the normal load be applied. We will assume that remote normal load is applied suddenly and homogeneously, i.e., that is of the form  $P = P_0 H(t)$ . In so doing, the interfacial normal traction is given by Eq. (3.10), and will comprise a two-wave structure, with a longitudinal head wave propagating away from the edge of the contact zone, followed by a slower transverse wave component (see Fig. 2a).

Imagine that concurrently with the normal load, an additional tangential load is applied on the material, and that is also of the form  $Q = Q_0 H(t)$ . Irrespective of the magnitude (and indeed, irrespective of the form) of the tangential load, any interfacial traction arising from the remote tangential load will necessarily propagate only at the transverse speed of sound. This means that in the spatial strip defined by the head wave, given by  $x \in [tc_l, tc_t], \forall t > 0$ , only the normal traction (which is non-singular in this region, as may be seen in Fig. 2a), has sufficient time to influence the interface.

As a result, the regions touched by the head wave will always remain trivially in full stick, because  $q(x, t) = 0$ . It also follows that

at any time, slip is only possible for  $x \in [0, tc_l]$ . Stick is guaranteed so long as  $|q(x, t)| \leq fp(x, t)$ . In considering the asymptotic form of  $p(x, t)$  and  $q(x, t)$ , we can infer that owing to the magnitude of the singularities at the edge of the contact interface, it is not necessarily the case that  $p(x, t)$  and  $q(x, t)$  will cancel one another. In particular, the near field, we ought to would expect a fully stuck solution so long as

$$K_{II}(t) \leq fK_I(t) \quad (3.17)$$

which is a condition analogous to the one found by Dini and Hills for the similar static near field (Dini and Hills, 2003). The relation

$$\frac{a}{b} = \frac{\sqrt{1-2\nu}}{\sqrt{2}\sqrt{1-\nu}}, \quad (3.18)$$

enables us to rewrite Eq. (3.17) as

$$Q_0 \leq fP_0 \Rightarrow \chi = \frac{fP_0}{Q_0} \geq 1 \quad (3.19)$$

where  $\chi$  is defined for convenience.

It is not immediately obvious that the asymptotic condition  $\chi \geq 1$  will be identically satisfied in the far field, owing to the fact that in the far field  $p(x, t)$  and  $q(x, t)$  are subjected to changes in sign relative to the base level. Hence, there is room for local slip in the far field, which travels in wave form. These region of local slip will be discussed in the sequel. We must also stress that the conditions of slip will be heavily dependent on the way the remote loading is applied. In the following, we shall always assume that the contact is applied as a result of a sudden *shock load*, whereby  $P = Q = 0$  for  $t < 0$ , and  $P = P_0$ ,  $Q = Q_0$  for  $t > 0$ . This is done in the interest of space, since there are infinitely many ways a steady state load of magnitude  $P_0$  (or  $Q_0$ ) may be reached when time is an explicit field variable. More complex time-dependent loading is nevertheless possible (e.g., the ramp loading considered in Gurrutxaga-Lerma, 2019). In the event the remote loading can be expressed as the product of a time dependent function  $P = P_0 f(t)$ ,  $Q = Q_0 g(t)$ , then the ensuing interfacial tractions (call them  $p^*(x, t)$  and  $q^*(x, t)$ ) can simply be obtained as time convolutions of the result we have presented here, as

$$p^*(x, t) = \langle P_0 \partial_t f(t), p(x, t) \rangle, \quad q^*(x, t) = \langle Q_0 \partial_t g(t), q(x, t) \rangle \quad (3.20)$$

where  $\langle \cdot, \cdot \rangle$  denotes convolution. The rest of considerations we laid out here would remain largely unchanged.

In the current shock loading scenario, if the remote load  $Q_0$  is sufficiently large and  $\chi < 1$ , however, there is no question that the

interface will have to slip so as to be able to satisfy the slip condition that  $|q(x, t)| = f \text{sign}(\dot{u}(x, t))p(x, t)$ . The magnitude of this relative slip can be calculated by introducing a corrective shear strain,  $s(x, t)$ , which helps ensure the slip condition that

$$|q(x, t) + s(x, t)| = -f \text{sign}(\dot{u}(x, t))p(x, t) \quad (3.21)$$

is satisfied. The corrective shear traction is the result of a certain slip distribution,  $u(x, t)$ , acting along the interface. Whilst expressions for  $q(x, t)$  and  $p(x, t)$  are available in the literature, the general expression for the  $s(x, t)$  'corrective' traction due to an arbitrary  $u(x, t)$  distribution of slip appears not to be available, and is derived in the sequel.

#### 4. Surface tractions due to a distributed displacement along the interface

This section aims at deriving the general expression for the interfacial tractions prompted by an arbitrary displacement distributed along a contact interface. For generality and completion, we shall derive the tractions due to a vertical displacement distribution  $u_y(x, t) \equiv v(x, t)$ , and due to a tangential displacement  $u_x(x, t) \equiv u(x, t)$ . That is,  $u(x, t)$  and  $v(x, t)$  are two arbitrary distributed displacements acting along the interface on the horizontal  $x$ -direction (mode I) and the vertical  $y$ -direction (mode II), respectively. We wish to find the interfacial tractions associated with each of them.

##### 4.1. Governing equations and solution strategy

The problem we wish to solve is governed by the equation of conservation of linear momentum acting along the interface. We place the interface along the abscissae axis at  $y = 0$ , and the edge of the contact at  $x = 0$ . For a linear isotropic medium, conservation takes the form of the Navier-Lamé equation (Achenbach, 1973):

$$(\lambda + \mu)u_{j,ji} + \mu u_{i,jj} = \rho \ddot{u}_i \quad (4.1)$$

where  $\lambda$  and  $\mu$  are respectively Lamé's first and second parameters,  $\rho$  the density,  $u_i$  the  $i$ th component of the displacement field,  $u_{i,j} = \partial_j u_i$  and repeated index denotes summation.

For a planar problem, we may define the  $\phi(x, y, t)$  and  $\psi(x, y, t)$  Kelvin-Helmholtz potentials such that (Eringen and Suhubi, 1975; Gurrutxaga-Lerma et al., 2015; 2013),

$$u_x = \frac{\partial \phi}{\partial x} - \frac{\partial \psi}{\partial y}, \quad u_y = \frac{\partial \phi}{\partial y} + \frac{\partial \psi}{\partial x} \quad (4.2)$$

Applying these two potentials to Eq. (4.1), one is able to separate it into two monochromatic wave equations:

$$\frac{\partial^2 \phi}{\partial x^2} + \frac{\partial^2 \phi}{\partial y^2} = a^2 \frac{\partial^2 \phi}{\partial t^2}, \quad \frac{\partial^2 \psi}{\partial x^2} + \frac{\partial^2 \psi}{\partial y^2} = b^2 \frac{\partial^2 \psi}{\partial t^2} \quad (4.3)$$

where  $a = \sqrt{\rho/(\lambda + 2\mu)} = 1/c_l$  and  $b = \sqrt{\rho/\mu} = 1/c_t$  are the longitudinal and transverse slownesses of sound, respectively, and  $c_l$  and  $c_t$  the longitudinal and transverse speeds of sound, respectively.

The problem we wish to solve consists of Eq. (4.3) under boundary conditions

$$\begin{aligned} u_x(x, 0, t) &= u(x, t) & x \in \mathbb{R}^+ \\ u_y(x, 0, t) &= v(x, t) & x \in \mathbb{R}^+ \end{aligned} \quad (4.4)$$

where  $u(x, t)$  and  $v(x, t)$  are the interfacial displacements we wish to find, which as stated we shall assume are sufficiently smooth (at least  $C^2(\mathbb{R}^+)$ ) and are supported over  $x \in \mathbb{R}^+$ .

Our solution strategy relies on two steps: First, we separate by superposition the two boundary value problems, so that each may be solved independently:

$$u_x(x, 0, t) = u(x, t) \quad x \in \mathbb{R}^+ \quad (4.5)$$

and

$$u_y(x, 0, t) = v(x, t) \quad x \in \mathbb{R}^+ \quad (4.6)$$

Second, we seek the fundamental solution (i.e., the Green's function) to each of these problems. This means we need to find the solution to

$$u_x^p(x, t) = \delta(x - x_0)\delta(t - t_0)\delta(y) \quad (4.7)$$

and

$$u_y^p(x, t) = \delta(x - x_0)\delta(t - t_0)\delta(y) \quad (4.8)$$

where  $x_0 > 0$ , so that  $u_x^p$  and  $u_y^p$  are non-zero only for  $x \in \mathbb{R}^+$ .

In finding the solution to Eqs. (4.7) and (4.8), we only need to look for the interfacial tractions, which we shall call  $p^p(x, t)$  and  $t^p(x, t)$  respectively. The actual interfacial tractions we wish to find are the solution to Eq. (4.4). Given that the fundamental solutions  $p^p(x, t)$  and  $t^p(x, t)$  are known, they can be obtained by reaching the representation formula (Evans, 2010), whereby

$$\begin{aligned} p(x, t) &= \int_{\mathbb{R} \times \mathbb{R}} u(x - x', t - t') p^p(x', t') dx' dt', \\ t(x, t) &= \int_{\mathbb{R} \times \mathbb{R}} v(x - x', t - t') t^p(x', t') dx' dt' \end{aligned} \quad (4.9)$$

Thus, invoking this representation formula, the interfacial tractions due to  $u(x, t)$  and  $v(x, t)$  may be obtained from the convolution of  $u(x, t)$  and  $v(x, t)$  with the tractions due to the point displacements  $u_x^p(x, t)$  and  $u_y^p(x, t)$  respectively, each acting along the interface.

The interfacial tractions due to  $u_x^p(x, t)$  and  $u_y^p(x, t)$  are the only unknowns, and correspond to deformations in mode I and mode II respectively, which we derive in the following.

##### 4.2. Fundamental solution to mode I

We begin with  $u_y^p(x, t)$  – exactly the same procedure would be followed for  $u_x^p(x, t)$ . The solution procedure will follow the usual Wiener-Hopf method (see Noble, 1958). The boundary value problem prescribed by Eq. (4.8) acts only on the positive real line. Most integral solution methods require the boundary conditions be applied on the whole real line. Following the Wiener-Hopf strategy, we shall extend  $u_y(x, 0, t)$  by continuity to  $\mathbb{R}^-$ . Given that the value of  $u_y(x, 0, t)$  for  $x < 0$  is unknown, this is achieved by introducing an unknown function  $u_-(x, t)$  supported on  $x \in \mathbb{R}^-$ , that will now form part of the solution we seek.

Equally, the boundary value problem is incomplete without detailing the stress state at the interface. In general, we shall require that

$$\sigma_{yy}(x, 0, t) = 0 \quad x \in \mathbb{R}^-, \quad \sigma_{xy}(x, 0, t) = 0 \quad x \in \mathbb{R} \quad (4.10)$$

which defines the free surface in the area not under contact. Again, as per Wiener-Hopf, we shall extend  $\sigma_{yy}(x, 0, t)$  by continuity to  $x \in \mathbb{R}^+$ .

The boundary value problem we wish to solve is

$$\begin{aligned} \sigma_{yy}(x, 0, t) &= p_+(x, t) & x \in \mathbb{R} \\ u_y(x, 0, t) &= u_-(x, t) + \delta(x - x_0)\delta(t - t_0)\delta(y) & x \in \mathbb{R} \\ \sigma_{xy}(x, 0, t) &= 0 & x \in \mathbb{R} \end{aligned} \quad (4.11)$$

where  $p_+(x, t)$  denotes the (unknown) normal stress along the contact interface, with compact support for  $x \in \mathbb{R}^+$ ; and  $u_-(x, t)$  denotes the unknown displacement at the free surface, offering compact support on  $x \in \mathbb{R}^-$ .

We define the following integral transforms, that will be applied in succession on Eq. (4.3) and the boundary conditions:

$$\hat{f}(x, y, s) = \int_0^\infty f(x, y, t) e^{-st} dt, \quad F(k, y, s) = \int_{-\infty}^\infty \hat{f}(x, y, s) e^{-skx} dx \quad (4.12)$$

We first transform the boundary conditions, leading to

$$\begin{aligned} \mu \left[ (b^2 - 2a^2)s^2 \Phi + 2 \frac{\partial^2 \Phi}{\partial y^2} - 2sk \frac{\partial \Psi}{\partial y} \right]_{y=0} &= \frac{P_+(k)}{s^2} \\ \mu \left[ 2sk \frac{\partial \Phi}{\partial y} + \frac{\partial^2 \Psi}{\partial y^2} - s^2 k^2 \Psi \right]_{y=0} &= 0 \\ \left[ \frac{\partial \Phi}{\partial y} - sk \Psi \right]_{y=0} &= \frac{1}{s^3} U_-(k) + e^{-s(t_0 + kx_0)} \end{aligned} \quad (4.13)$$

where

$$\begin{aligned} P_+(k) &= s^2 \int_{-\infty}^{\infty} \hat{p}_+(x, y, s) e^{-skx} dx \\ U_-(k) &= s^3 \int_{-\infty}^{\infty} \hat{u}_-(x, y, s) e^{-skx} dx \end{aligned} \quad (4.14)$$

The governing Eqs. (4.3) are also transformed, rendering

$$\frac{\partial^2 \Phi}{\partial y^2} = \alpha(k)^2 s^2 \Phi, \quad \frac{\partial^2 \Psi}{\partial y^2} = \beta(k)^2 s^2 \Psi \quad (4.15)$$

where  $\alpha(k) = \sqrt{a^2 - k^2}$  and  $\beta(k) = \sqrt{b^2 - k^2}$ .

The solutions to Eq. (4.15) will be of the form  $\Phi(k, y, s) = C_\phi(s, k) e^{-\alpha(k)y}$  and  $\Psi(k, y, s) = C_\psi(s, k) e^{-\beta(k)y}$ , where  $C_\phi(k, s)$ ,  $C_\psi(k, s)$  are the integration constants, in principle to be determined through the boundary conditions.

Upon substituting the solutions into the system of equations established by the boundary conditions (Eq. (4.13)), we find ourselves with three equations and four unknowns. We can nonetheless reduce the system to an equation relating  $U_-(k)$  with  $P_+(k)$  – the two unknown variables we are most interested in:

$$P_+(k) = -\frac{\mu}{b^2} \frac{R(k)}{\alpha(k)} (U_-(k) + s^3 e^{-s(t_0 + kx_0)}) \quad (4.16)$$

where

$$R(k) = (b^2 - 2k^2)^2 + 4\alpha\beta k^2 \quad (4.17)$$

is the Rayleigh function (cf. Achenbach, 1973). This is the Wiener-Hopf equation of the problem.

The Wiener-Hopf method will now attempt to factorise this equation into sectionally analytic functions over the positive and negative real lines. This is done because if the factorisation is successful, then Eq. (4.16) will establish an equality between sectionally holomorphic functions in  $x \in \mathbb{R}^-$  and in  $x \in \mathbb{R}^+$ . If that is the case, then by Liouville's generalised theorem (see Markushevich, 2005) each part of the equality must be equal to a polynomial, which facilitates the solution we seek.

The Wiener-Hopf factorisation proceeds as follows. We first perform a product factorisations for the  $\alpha(k)$  and  $R(k)$  functions, which is standard (cf. Achenbach, 1973; Miklowitz, 1978). Thus, if we write

$$\alpha(k) = \alpha_+(k) \cdot \alpha_-(k), \quad \alpha_\pm(k) = \sqrt{a \pm k} \quad (4.18)$$

We achieve a successful factorisation of  $\alpha$  into sectionally analytic functions, since  $\alpha_+(k)$  is analytic for  $|k| > a$  and  $\alpha_-(k)$  for  $|k| < a$ .

The factorisation of  $R(k)$  is also standard (Achenbach, 1973; Freund, 1998). We introduce the auxiliary function

$$S(k) = \frac{R(k)}{2(b^2 - a^2)(c^2 - k^2)} \quad (4.19)$$

with  $c = 1/c_R$ . This is factorised as  $S(k) = S_+(k) \cdot S_-(k)$ , where (Achenbach, 1973)

$$\ln S_\pm(k) = -\frac{1}{\pi} \int_a^b \arctan \left[ \frac{4u^2 \sqrt{(u^2 - a^2)(b^2 - u^2)}}{(b^2 - 2u^2)^2} \right] \frac{du}{u \pm k} \quad (4.20)$$

Thus,

$$R_\pm(k) = 2(b^2 - a^2)(c \pm k)S_\pm(k) \quad (4.21)$$

Substituting into Eq. (4.16),

$$\begin{aligned} P_+(k) &= -\frac{\mu}{b^2} \frac{2(b^2 - a^2)(c + k)S_+(k)(c_R - k)S_-(k)}{\alpha_+(k)\alpha_-(k)} \\ &\quad \times (U_-(k) + s^3 e^{-s(t_0 + kx_0)}) \end{aligned} \quad (4.22)$$

leading to

$$\frac{P_+(k)}{F_+(k)} = -\frac{2\mu(b^2 - a^2)}{b^2} F_-(k) (U_-(k) + s^3 e^{-s(t_0 + kx_0)}) \quad (4.23)$$

where

$$F_\pm(k) = (c_R \pm k) \frac{S_\pm(k)}{\alpha_\pm(k)} \quad (4.24)$$

Thus, Eq. (4.16) has almost completely been factorised into sectionally analytic functions. What remains is the additive factorisation of  $F_-(k)s^3 e^{-s(t_0 + kx_0)}$ , which would be trivial to achieve were not for the exponential term in the expression. The exponential term  $e^{-s(t_0 + kx_0)}$  pertains to the  $t_0 > 0$  delay and the  $x_0 > 0$  offset in the application of the point displacement. This term has the unfortunate property of making the  $F_-(k)s^3 e^{-s(t_0 + kx_0)}$  term unbounded for  $|k| \rightarrow -\infty$ . This is because  $S_+(k) \rightarrow 1$  in that limit, so the convergence of the integrand is therefore dominated by this exponential term. A similar situation was noted by Georgiadis and Charalambakis (1994) in their study of mode I crack face loading in thin strips. Although equally present in his derivation of the interfacial stress field due to a point load applied on the crack face, (Broberg, 1999, p.454) incorrectly assessed that this sort of exponential terms did not lead to an unbounded behaviour, and proceeded to invoke Liouville's generalised theorem in a derivation that must therefore be regarded as suspect.

If any of the terms in the Wiener-Hopf equation is not bounded, Liouville's generalised theorem is not satisfied, which bars a direct application of the analytic continuation argument used in the Wiener-Hopf technique. The solution in this case can still be attained as described by Georgiadis and Charalambakis (1994), by direct integration of the semi-factorised equation. Thus, we divide each term in Eq. (4.23) by  $2\pi i(z - k)$  and integrate over  $z \in (-i\infty, +i\infty)$ ,

$$\begin{aligned} \frac{1}{2\pi i} \int_{-i\infty}^{+i\infty} \frac{P_+(z)}{F_+(z)} \frac{dz}{z - k} &= -\frac{2\mu(b^2 - a^2)}{b^2} \\ &\quad \times \left[ \frac{1}{2\pi i} \int_{-i\infty}^{+i\infty} \frac{F_-(z)U_-(k)}{z - k} \frac{dz}{z - k} + \frac{1}{2\pi i} \int_{-i\infty}^{+i\infty} \frac{s^3 F_-(z)e^{-s(t_0 + kx_0)}}{z - k} \frac{dz}{z - k} \right] \end{aligned} \quad (4.25)$$

We can formally find the value of each of these integrals. The integral in the left hand side may be evaluated by closing an integration contour along the imaginary axis with a semi-circle along the positive half plane the radius of which we set tending to infinity. The sole pole due to  $F_+(z)$  is  $k = -c_R$ , located on the negative half plane, as are all branch cuts. Hence, pole and branch cuts are avoided by the closed contour formed by the semi-circle and the imaginary axis. Finally, the asymptotic behaviour of  $P_+(k)$  at infinity may be guessed from the expectation that  $p_+(x, t) \sim 1/\sqrt{x}$  for  $x \rightarrow 0^+$ ; invoking the Tauberian theorem (cf. Wiener, 1988), we have that  $P_+(k) \sim 1/k$  for  $|k| \rightarrow \infty$ . This means that the contribution of the circular segments vanishes by Jordan's lemma. Thus, Cauchy's theorem holds and

$$\frac{1}{2\pi i} \int_{-i\infty}^{+i\infty} \frac{P_+(z)}{F_+(z)} \frac{dz}{z - k} = \frac{1}{2\pi i} \oint \frac{P_+(z)}{F_+(z)} \frac{dz}{z - k} = \frac{P_+(k)}{F_+(k)} \quad (4.26)$$

The first integral in the right hand side follows similarly. In this case,  $u_-(x, t) \sim x^{1/2}$  for  $x \rightarrow 0^+$ , so that by the Tauberian theorem,

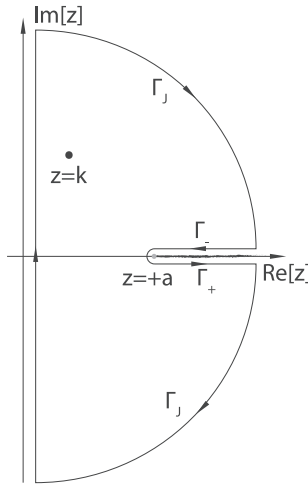


Fig. 3. Integration contour.

$U_-(k) \sim k^{-3/2}$  vanishes for  $|k| \rightarrow \infty$ . This enables us to close the integration contour along the imaginary axis with a semi-circle tending to infinity along the negative half plane, so that the semi-circle's contribution vanishes as well. The integrand has a pole at  $k = +a$ , and a branch cut is defined for  $\text{Re}[k] > a$ . Thus, the branch cut and both the  $k = +a$  and the  $z = k$  poles are avoided when closing the contour along the negative half plane, which leads us to conclude that by virtue of Cauchy's integral theorem

$$\frac{1}{2\pi i} \int_{-i\infty}^{i\infty} F_-(k) U_-(k) \frac{dz}{z-k} = 0 \quad (4.27)$$

The only remaining integrand may be evaluated as follows. Take

$$\frac{1}{2\pi i} \int_{-i\infty}^{i\infty} s^3 F_-(z) e^{-s(t_0 + z x_0)} \frac{dz}{z-k} \quad (4.28)$$

We begin by considering the closed contour on the positive half plane schematically represented in Fig. 3. In the positive half plane, the integrand vanishes for  $|z| \rightarrow \infty$ , so the contribution of the Jordan contours  $\Gamma_J$  vanishes (note this is not the case in the negative half plane). The only complication is that the integrand has poles at  $z = k$  and  $z = a$  with a branch cut along  $\text{Re}[z] > a$ . Thus, we need to avoid the branch cut along the real axis as indicated in Fig. 3, with a dual contour above and below the real axis from  $\text{Re}[z] \in [a, \infty)$ . In closing the contour of integration and invoking Cauchy's integral theorem (cf. Markushevich, 2005), only the pole at  $z = k$  remains inside the integral, whereupon

$$\begin{aligned} & \frac{1}{2\pi i} \int_{-i\infty}^{i\infty} s^3 F_-(z) e^{-s(t_0 + z x_0)} \frac{dz}{z-k} \\ &= s^3 e^{-s(t_0 + k x_0)} F_-(k) - \frac{1}{2\pi i} \int_{\Gamma_- + \Gamma_+} s^3 F_-(z) e^{-s(t_0 + z x_0)} \frac{dz}{z-k} \end{aligned} \quad (4.29)$$

where  $\Gamma_- = (\infty, a]$ ,  $\Gamma_+ = [a, \infty)$ .

The integrals along  $\Gamma_{\pm}$  cancel one another. Indeed, if we set  $z - a = r e^{i\theta}$  for  $\theta = 0$  along  $\Gamma_-$  and  $\theta = 2\pi$  along  $\Gamma_+$ , so that  $\Gamma_- \equiv r \in (\infty, 0]$ ,  $\Gamma_+ \equiv r \in [0, \infty)$ , we find that

$$\begin{aligned} & \int_{\Gamma_-} \frac{c_R + a - r(\cos \theta + i \sin \theta)}{a + r(\cos \theta + i \sin \theta) - z} r^{-1/2} \\ & \times \left( \cos \left( \frac{\theta}{2} \right) + i \sin \left( \frac{\theta}{2} \right) \right) S_-(a + r(\cos \theta + i \sin \theta)) dr \Rightarrow \int_{\Gamma_-} = - \int_{\Gamma_+} \end{aligned} \quad (4.30)$$

upon changing  $\theta = 0$  for  $\theta = 2\pi$ .

Thus, we finally recover the following sectionally analytic equation:

$$\begin{aligned} \frac{P_+(k)}{F_+(k)} &= - \frac{2\mu(b^2 - a^2)}{b^2} s^3 e^{-s(t_0 + k x_0)} F_-(k) \Rightarrow P_+(k) \\ &= - \frac{2\mu(b^2 - a^2)}{b^2} s^3 e^{-s(t_0 + k x_0)} F(k) \end{aligned} \quad (4.31)$$

where

$$\begin{aligned} F(k) &= \frac{1}{2(b^2 - a^2)} \frac{R(k)}{\alpha(k)} = \frac{1}{2(b^2 - a^2)} \\ & \times \left[ \underbrace{\frac{(b^2 - 2k^2)^2}{\alpha(k)}}_{A(k)} + \underbrace{4\beta(k)k^2}_{B(k)} \right] = \frac{1}{2(b^2 - a^2)} [A(k) + B(k)] \end{aligned} \quad (4.32)$$

The inversion of Eq. (4.32) may be achieved using the Cagniard-de Hoop technique (De Hoop, 1960; Cagniard, 1939) as follows. Consider the first (spatial) inversion integral (in Laplace space):

$$\hat{p}(x - x_0, s) = - \frac{\mu}{b^2} s e^{-s t_0} \frac{1}{2\pi i} \int_{-i\infty}^{i\infty} F(k) e^{s k (x - x_0)} s dk \quad (4.33)$$

The  $A(k)$  term in the integrand (see Eq. (4.32)) has poles at  $k = \pm a$  and branch cuts for  $|\text{Re}[k]| < a$ . The second term, containing  $B(k)$ , has no poles, but it does have a branch cut for  $|\text{Re}[k]| > b$ . The integration path may be closed with a semi-circular contour along the negative half plane for  $(x - x_0) > 0$  and along the positive half plane for  $(x - x_0) < 0$  (see Fig. 4).

Closure of the contour is provided on either the positive or negative half plane depending on the value of  $x$  relative to  $x_0$  (i.e.,  $(x - x_0)$ ) so that we can ensure that Jordan's lemma guarantees that the integral along the semi-circular contours vanish in the  $R \rightarrow \infty$  limit; this requires that  $(x - x_0) > 0$ . Irrespective of whether the contour is closed along the positive or negative half plane, the branch cuts (and the pole) of each of the two terms in the integrand must be avoided in a manner analogous to how the branch cut was avoided in Fig. 3. In so doing, there are no poles remaining inside the closed contour, so by Cauchy's theorem (cf. Markushevich, 2005) the integral along the imaginary axis is of the same value as that encircling the branch cuts.

The integral along the branch cuts may be evaluated by setting  $\tau = -k(x - x_0)$ , with  $d\tau = -(x - x_0)dk$ , so that  $\Gamma_t \equiv \tau \in [a|x - x_0|, \infty)$  for  $A(k)$ , and  $\Gamma_t \equiv \tau \in [b|x - x_0|, \infty)$  for  $B(k)$ . Applying Schwarz's reflection principle (see Markushevich, 2005), we find that

$$\begin{aligned} \hat{p}(x - x_0, s) &= - \frac{s^2 e^{-s t_0}}{\pi(x - x_0)} \left[ \int_{a(x - x_0)}^{\infty} \text{Im} \left[ A \left( - \frac{\tau}{x - x_0} \right) \right] e^{-s \tau} d\tau \right. \\ & \left. + \int_{b(x - x_0)}^{\infty} \text{Im} \left[ B \left( - \frac{\tau}{x - x_0} \right) \right] e^{-s \tau} d\tau \right] \end{aligned} \quad (4.34)$$

Applying the Bromwich integral and the properties of the Laplace transform, we finally obtain that

$$\begin{aligned} p(x, t) &= \frac{\mu}{b^2 \pi} \frac{1}{x^4} \\ & \times \left[ \frac{a^2 b^2 x^6 (b^2 - 8a^2) - 60a^2 t^4 x^2 + 2t^2 x^4 (24a^4 - 2a^2 b^2 + b^4) + 24t^6}{(t^2 - a^2 x^2)^{5/2}} \right. \\ & \left. \times H(t - a|x|) + \frac{4(2b^4 x^4 - 9b^2 t^2 x^2 + 6t^4)}{(t^2 - b^2 x^2)^{3/2}} H(t - b|x|) \right] \end{aligned} \quad (4.35)$$

where  $x - x_0$  and  $t - t_0$  have been substituted for  $x$  and  $t$  respectively for brevity.



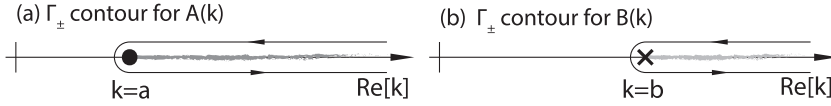


Fig. 4. Integration contours for the Cagniard-de Hoop inversion of Eq. (4.31) and  $x - x_0 < 0$ .

#### 4.3. Fundamental solution to mode II

In this case,  $u_x^p = \delta(x - x_0)\delta(t - t_0)\delta(y)$ . Using exactly the same strategy as for mode I, the boundary value problem to solve is:

$$\begin{aligned} \sigma_{xy}(x, 0, t) &= t_+(x, t) & x \in \mathbb{R} \\ u_x(x, 0, t) &= u_-(x, t) + \delta(x - x_0)\delta(t - t_0)\delta(y) & x \in \mathbb{R} \\ \sigma_{yy}(x, 0, t) &= 0 & x \in \mathbb{R} \end{aligned} \quad (4.36)$$

where  $t_+(x, t)$  is the unknown interfacial shear traction we wish to find, offering compact support for  $x \in \mathbb{R}^+$ , and  $u_-(x, t)$  the unknown free surface displacements, with compact support over  $x \in \mathbb{R}^-$ . The solution procedure is analogous to mode I, and will not be repeated here. As before, Liouville's theorem cannot be directly applied and an analogous reasoning to mode I's must be followed to reach the equation

$$T_+(k) = -\frac{\mu}{b^2} \frac{R(k)}{\beta(k)} s^3 e^{-s(t_0 + kx_0)} \quad (4.37)$$

which may be inverted using Cagniard-de Hoop to get:

$$\begin{aligned} t(x, t) = \frac{\mu}{b^2 \pi x^4} & \left[ \frac{-7b^6 x^6 + 46b^4 t^2 x^4 - 60b^2 t^4 x^2 + 24t^6}{(t^2 - b^2 x^2)^{5/2}} H(t - b|x|) \right. \\ & \left. + \frac{4(2a^4 x^4 - 9a^2 t^2 x^2 + 6t^4)}{(t^2 - a^2 x^2)^{3/2}} H(t - a|x|) \right] \end{aligned} \quad (4.38)$$

#### 4.4. Distribution of slip

The kernel functions  $p(x, t)$  and  $t(x, t)$  enable us to express the interfacial normal and shear tractions due to the  $u(x, t)$  and  $v(x, t)$  displacement distributions as the convolutions  $s_I(x, t) = p(x, t) \star u(x, t)$  and  $s_{II}(x, t) = t(x, t) \star v(x, t)$  where  $\star$  denotes temporal and spatial convolution. The kernel functions in both cases are hypersingular. In order to regularise them, we first express the displacements as a convolution of step functions (Aki and Richards, 2002),

$$\begin{aligned} u(x, t) &= \int_0^\infty \int_0^\infty \frac{\partial^2 u}{\partial t' \partial x'} H(x - x') H(t - t') dx' dt', \\ v(x, t) &= \int_0^\infty \int_0^\infty \frac{\partial^2 v}{\partial t' \partial x'} H(x - x') H(t - t') dx' dt' \end{aligned}$$

By the properties of the convolution, and setting  $u_{xt}''(x, t) = b_x(x, t)$  and  $v_{xt}'' = b_y(x, t)$ , and  $P(x, t) = \int \int p(x, t) dx dt$  and  $T(x, t) = \int \int t(x, t) dx dt$ , we can write  $s_I(x, t) = P(x, t) \star b_x(x, t)$  and  $s_{II}(x, t) = Q(x, t) \star b_y(x, t)$ , that is

$$\begin{aligned} s_I(x, t) &= \frac{\mu}{b^2 \pi} \int_0^x \int_0^t \left[ -\frac{(b^2 x'^2 - 2t'^2)^2}{t' x'^3 \sqrt{t'^2 - a^2 x'^2}} H(t' - ax') \right. \\ & \quad \left. - \frac{4t' \sqrt{t'^2 - b^2 x'^2}}{x'^3} H(t' - bx') \right] b_y(x - x', t - t') dt' dx' \end{aligned} \quad (4.39)$$

$$\begin{aligned} s_{II}(x, t) &= \frac{\mu}{b^2 \pi} \int_0^x \int_0^t \left[ -\frac{(b^2 x'^2 - 2t'^2)^2}{t' x'^3 \sqrt{t'^2 - b^2 x'^2}} H(t' - bx') \right. \\ & \quad \left. - \frac{4t' \sqrt{t'^2 - a^2 x'^2}}{x'^3} H(t' - ax') \right] b_x(x' - x, t - t') dt' dx' \end{aligned} \quad (4.40)$$

We note that  $b_x(x, t)$  and  $b_y(x, t)$  are a velocity density gradient for the slip along the  $y$  and  $x$  directions, respectively.

#### 4.4.1. Corrective shear traction at the contact interface

It would appear that the integrals remain hypersingular at the origin. However, some simple manipulations facilitate dealing with the kernels. Given that the core concern of the method lies on the  $s_{II}(x, t)$  distribution, we shall focus on its regularisation; the one for  $s_I(x, t)$  can be achieved in a similar fashion.

Let us therefore introduce the following transformation:

$$x \mapsto x, \quad t \mapsto u \cdot x \quad (4.41)$$

with Jacobian

$$|J| = \begin{vmatrix} \frac{\partial x}{\partial x} & \frac{\partial x}{\partial u} \\ \frac{\partial t}{\partial x} & \frac{\partial t}{\partial u} \end{vmatrix} = x$$

so that  $dt = x du$ .

Applying the transformation on  $s_{II}(x, t)$  we find that the kernels become

$$\begin{aligned} K_b(x, u) &= -\frac{(b^2 - 2u^2)^2}{u \sqrt{u^2 - b^2}} H(x(u - b)), \\ K_a(x, u) &= -4u \sqrt{u^2 - a^2} H(x(u - a)) \end{aligned} \quad (4.42)$$

Note that the kernel functions do not depend on  $x$  for  $x > 0$ . It can therefore be written that:

$$\begin{aligned} s_{II}(x, u) &= \frac{\mu}{b^2 \pi} \left[ \int_{\Gamma_a} K_a(u - u') B(u'; x') du' \right. \\ & \quad \left. + \int_{\Gamma_b} K_b(u - u') B(u'; x') du' \right] \end{aligned} \quad (4.43)$$

where

$$\Gamma_a = [0, u - a], \quad \Gamma_b = [0, u - b] \quad (4.44)$$

and

$$B(u; x) \equiv \dot{u}(u; x) = \int_0^x b_x(u, x - x') dx' \quad (4.45)$$

is the particle velocity. This regularises the problem and, furthermore, simplifies the convolution integral by making the kernels depend solely on  $u$  'velocity' variable. The ability to write down the kernels in this fashion comes down to the fact that the interfacial problem is in effect self-similar, i.e., homogeneous to degree 0 in  $x$  and  $t$  (Eringen and Suhubi, 1975) – similar results were observed by Kostrov for antiplanar problems (Kostrov, 1964), and are discussed at greater length by Eringen and Suhubi (1975).

#### 5. Solution to the contact problem

Having derived the interfacial tractions due to the shearing load, the normal load, and the interfacial slip, we are in a position to study the resulting mechanical equilibrium across the interface, for the region about the edge of the contact zone. Given the hyperbolic nature of the system, the solution will consist of propagating loads in and from the interface.

Under slip conditions, the force balance at the interface requires

$$|q(x, t) + s_{II}(x, t)| = -f \text{sign}(f) p(x, t) \quad (5.1)$$

subject to the provisions described in Section 2, so that

$$\text{sign}(f) = \frac{\dot{u}(x, t)}{|\dot{u}(x, t)|}$$

is the sign of the friction force. An analytic solution to Eq. (5.1) does not appear to be available (Vainikko, 1993).

### 5.1. Numerical algorithm

A detailed implementation of the numerical algorithm employed to solve the integral Eq. (5.1) is given in Appendix B. There we detail how, using a Nyström-collocation method (Porter and Stirling, 1990; Atkinson, 1997), upon discretising the problem, it is possible to solve the equation as a matricial problem of the form

$$F_k = b_j L_{jk} \quad (5.2)$$

where  $F_k$  is a vector of forces,  $b_j$  the unknown coefficients of some basis set, and  $L_{jk}$  the time-dependent kernel. Both  $F_k$  and  $L_{jk}$  can be computed a priori:  $F_k$  are the values of the  $q(u) - f \text{sign}(\dot{v})p(u)$  interfacial force vector evaluated at the collocation point  $u_k$ , and  $L_{jk}$  the nodal values of the convolution of  $K_a(u) + K_b(u)$  with a triangular basis function (see the Appendix B for further details). The system in Eq. (5.2) is solved for  $b_j$ , whereupon the desired solution can be reconstructed as

$$B_x(u) = \sum_{i=0}^{n_u} \sum_{b=0}^{n_u} b_j N_j(u) \quad (5.3)$$

for

$$N_j^\Lambda(u) = \begin{cases} \frac{u-u_{j-1}}{u_j-u_{j-1}} & u \in [u_{j-1}, u_j] \\ \frac{u_{j+1}-u}{u_{j+1}-u_j} & u \in [u_j, u_{j+1}] \\ 0 & \text{otherwise} \end{cases} \quad (5.4)$$

a standard triangular basis function (Atkinson, 1997).

## 6. Results and discussion

The aim of this section is to study how the slip region evolves over time as a result of the dynamic loading conditions. We consider only the time-dependent part of the elastodynamic solutions – any time-independent contribution could be added by superposition to the time-dependent part. We use the  $\chi = fP_0/Q_0$  parameter to discriminate between different loading regimes, and draw distinctions between known loading regimes in the static case (Barber, 2018). Thus, in the following we will examine the form and evolution of the slip region, which as outlined in Section 3.6 speaking should be expected to evolve if  $\chi \leq 1$ . Unless otherwise stated, we will take  $a = 0.1$ ,  $b = 0.05$  (implying  $c_l = 10$ ,  $c_t = 5$ ,  $c_R = 4.662$ , and a Poisson ratio of  $\nu = 1/3$ ),  $f \cdot P_0 = 1$ , and  $Q_0 = 1/\chi$ . The aim of this section is to elucidate how the slip region evolves over time as a result of the sudden loading of the interface. The  $\chi$  parameter is used to demarcate different loading regimes.

### 6.1. Anomalous slip for $\chi > 1$

In principle, for  $\chi > 1$  we should expect a fully stuck solution (Barber, 2018). However, owing to the transient nature of both  $q(x, t)$  and  $p(x, t)$ , it appears unlikely that  $|q(x, t)| \leq -fp(x, t)$  throughout the interface as the tangential and normal loads propagate inward. In particular, we find that in the environs of the shear wave front (i.e., for values of  $x$  close to  $c_t t$ ),  $fp(x, t)$  is likely to be smaller than the corresponding  $q(x, t)$ , thereby violating the stick requirement. Under these conditions, an anomalous region of slip – in reality, a slip wave – arises. This anomalous slip wave can be inferred from Fig. 5, which depicts the interfacial tangential velocity needed to accommodate the imbalance. As can be seen, as the friction coefficient is increased, this region of imbalance behind the shear wave front appears to narrow to a stable region which for sufficiently high  $\chi$ , is bounded to around  $x \approx \frac{b}{a} c_t t$  to  $x = c_t t$ .

The anomalous slip wave travels away from the edge of the contact zone, where stick is reestablished as expected from the asymptotic analysis provided in Section 3.6. Thus, over sufficient

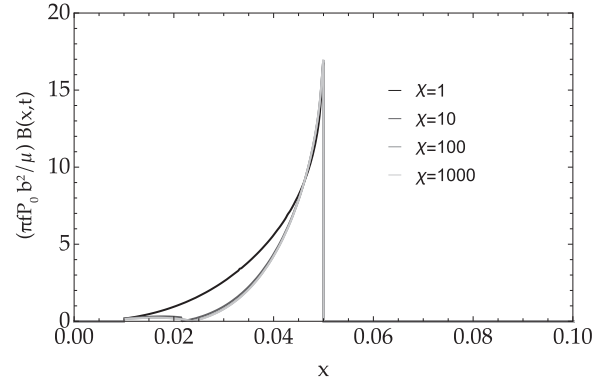


Fig. 5. Interfacial slip velocity for  $\chi > 1$ , which demarcates the anomalous slip wave traveling through the contact interface (in this case, at  $t = 0.01$ ).

timescales full stick is achieved, and the expected quasistatic fully stuck solution (cf. Hills and Nowell, 1994; Dini et al., 2005; Dini and Hills, 2004; Dini and Hills, 2003) is restored. However, under the dynamic loading conditions under consideration here, the anomalous slip wave appears unavoidable irrespective of the magnitude of the friction coefficient, or of how small  $Q_0$  might be. Thus, this result suggests that changes in the tangential loads under full stick conditions will inevitably be accompanied by a transient slip wave that travels away from the edge of the contact zone. The conditions leading to it are nonetheless heavily dependent on the frictional law and on the lack of additional damping mechanisms that may result in its attenuation or full dissipation. If such conditions are not present, the anomalous slip wave would entail surface vibrations and, as a result of the presence of additional slip, negatively impact the wear performance of the contacting interfaces.

### 6.2. Partial slip for $\chi < 1$

Conventional partial slip is observed for values of  $\chi < 1$ . The region of slip is confined to the strip between the edge of the contact zone and the rear of the head wave (i.e.,  $x \in [0, tc_l]$ ). As stated, this is because the longitudinal head wave is not accompanied by a tangential load, so for  $x \in [tc_l, tc_l]$  the interface remains trivially under full stick. As can be seen in Fig. 6, the slip region is marked by the presence of a maximum slip that considerably lags behind the shear wave front, and is also dependent on the  $\chi$  ratio. The maximum of slip is present strictly for  $\chi < 1$ , as that changes the character of the  $fp(x, t) - q(x, t)$  from convex to concave in the shear wave region. It is observed to increase in magnitude (alongside the rest of the slip distribution, Fig. 6b) as  $\chi$  decreases in magnitude, which is reasonable as the latter entails increasingly large tangential loads (or lower friction coefficients) that need larger slip to be accommodated.

Under the current loading, no natural limit to the slip zone is observed. This is because the magnitude of the elastodynamic loads is unbounded in time: as was noted in the asymptotic analysis of the normal and tangential stress distributions (Section 3.6), the intensity of the interfacial loads is monotonically increasing with  $\sqrt{t}$  at the edge of the contact zone, and this extends to the rest of the solution (cf. Broberg, 1999). This means that over time the normal and tangential loads keep increasing in magnitude and, as would also be the case in quasistatic problems, the width of the slip zone keeps increasing. In this case this happens not because  $\chi$  has varied, but because the interfacial tractions have, irrespective of  $\chi$ . Paradoxically, this entails that the  $t \rightarrow \infty$  limit does not recover the quasistatic solution – this can only be achieved through rarefaction (cf. Broberg, 1999). For that to happen, we would need to allow for the interface to interact with remote boundaries that

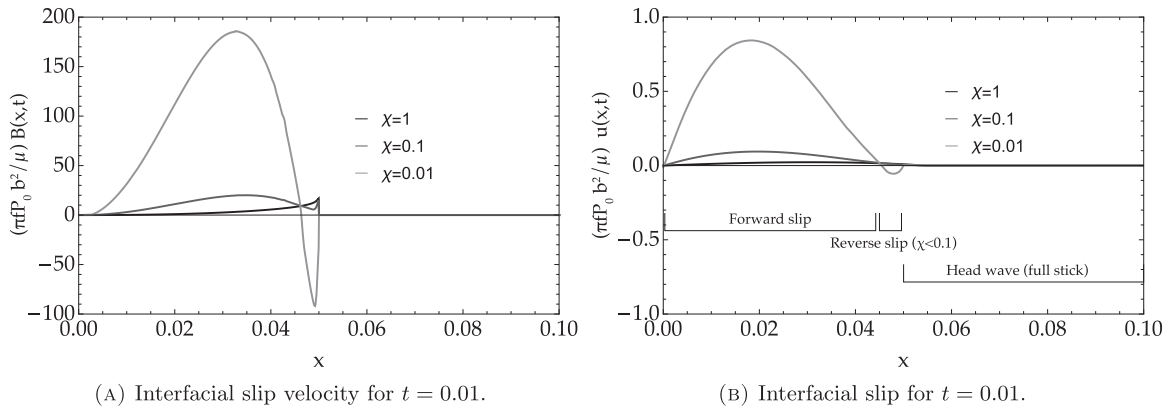


**Fig. 6.** Interfacial slip velocities and displacements for  $\chi < 1$  at  $t = 0.01$ . The head wave region encompasses  $x \in [0.05, 0.1]$ , and the Rayleigh wave is located in  $x \in [0.0466, 0.05]$ , where for sufficiently low  $\chi$  a region of reverse slip can be observed.

are not present in a semi-infinite plane. This means that the solutions presented in this semi-infinite interfacial analysis are of interest mainly for short time-scales, as would be attained in finite bodies for which the initial waves emitted from the edge of the contact zone have not been allowed to reach other free surfaces, be reflected inwards ('rarefaction') and reach the interface anew. Such problem is part of the more complex problem that would be posed by the presence of free surfaces. The elastic waves originally radiated away from the contact interface would eventually reach the free surfaces of the bodies, whereupon they would be reflected back towards the interface. This rarefaction phenomenon would potentially result in the relaxation of the interfacial stresses. This problem would be solvable as a superposition of the current problem alongside the interfacial tractions due to the rarefaction waves. Thus, rarefaction events would repeat themselves over time, increasing the mathematical complexity of the analysis, whilst the fundamental insights achieved through the solution to the current problem would remain in place.

The present results show that in the elastodynamic contact problem, slip propagates as a transverse wave across the interface. These slip waves exist irrespective of the values taken by the remote loads and the friction coefficient, although for  $\chi > 1$  they lead to a fully stuck solution over time. This is because shear and frictional loads are never fully balanced away from asymptotic considerations that only apply in the near field of the edge of the contact zone. No instability inherent to these slip wave is observed. This is in agreement with prior observations that Adams-like instabilities are promoted only for fully coupled and/or dissimilar materials (Adams, 1995; 1998): neither is the case in the present analysis, so such instabilities should not be expected. Furthermore, in this case the driving force for the interfacial motions is remotely applied loads, not a prescribed uniform motion of the contacting blocks – to put it otherwise, the present problem is force controlled, not displacement controlled, so the slip wave is allowed to contribute to the relaxation of remote loading, and does not arise because of the need to relax singularities and tractional imbalances at a moving interface, which may lead to instability. The significance that the contact interface elastically runs along elastically similar bodies cannot be understated, since it in fact appears to prevent fully coupled deformations. Indeed, if one examines the mathematical form of the half space Green's functions (Eq. (3.3) for the case when  $y = 0$ , but reproduced fully in Eringen and Suhubi, 1975, p.615), we noted that  $u_x(x, y, t)$  (obtained from Eq. (3.5)) must be odd in  $y$ , and  $u_y(x, t)$  even. This means that  $u_{xy}$  is even in  $y$ , and so is  $\sigma_{xy}$ . It also follows that  $\sigma_{xx}$  and  $\sigma_{yy}$  must be odd in  $y$ . Crucially,  $\sigma_{yy}$  is odd and  $\sigma_{yy} = 0$  at the

interface, which entails that a  $u_x$  displacement is unable, by symmetry, to induce a  $\sigma_{yy}$  displacement. That is to say, the problem is uncoupled because the materials at either side of the interface are the same. Future work will focus on extending the approach to dissimilar materials, in the expectation that in so doing the fully coupled problem will be studied. In the present analysis, because the interface runs along elastically similar materials no Schallamach waves (Schallamach, 1971) will be formed (Barquins, 1985).

### 6.3. Reverse slip regime

A remarkable feature of the transient slip region captured here is that reverse slip (relative to reference) is observed to occur, as is shown in Fig. 6b, which depicts a region of reverse slip, alongside the companion slip velocity in Fig. 6a, which also displays the expected sign reversal for reverse slip to happen. The presence of reverse slip is observed to happen in particularly unfavourable conditions, as the  $\chi$  parameter decreases below  $\chi < 0.1$ . In these particular calculations, the limit is found to be at  $\chi = 0.0575$ ; below this value the slip interface is observed to divide between two distinct regions (see Fig. 6b for  $\chi = 0.01$ ): for  $x \in [0, t_{cR}]$ , conventional or forward slip governs the interfacial mechanics. In this region, both slip and velocities are positive. For  $x \in [t_{cR}, t_{cI}]$ , i.e., in the region between the Rayleigh wavefront and the transverse wave front, the interface undergoes reverse slip: both slip and interfacial velocities are negative (relative to reference, see Fig. 6).

Although dependent on the  $\chi$  parameter, the reverse slip region is an inherent feature of the interfacial mechanics. This is because the sign of the interfacial velocity is reversed due to the kernel of the corrective traction: so long as the balance between the applied normal and tangential forces is such that the tangential load is considerably larger (in relative terms) to the frictional force, the arrival of the Rayleigh wave will be marked by a sign reversal in the interfacial tractions that is transferred to the interfacial slip and velocities. This situation is mathematically analogous to the sign reversal observed in the fields of moving edge dislocations (Brock, 1982; Gurrutxaga-Lerma, 2018; Gurrutxaga-Lerma et al., 2015), where the stress fields of dislocations reverse their sign when the dislocations move with speeds higher than the Rayleigh wave speed. In both cases, it is the elastodynamic kernel that causes the sign reversal because of the need to accommodate for the slower Rayleigh (surface) waves. Sign reversals associated with the Rayleigh wave speed were also reported by Brock and Georgiadis (1994) in their study of interfacial tractions involved in the uniformly moving wedge-like indenter; although in both cases the sign reversal exists to accommodate the Rayleigh waves, in

their case the indenter was externally driven to penetrate the body at that speed, whereas in our case the two contacting bodies are driven by external forces, and there is no inherent sliding.

The reverse slip region will invariably broaden in space as time advances, but as the Rayleigh wave arrives at the interfacial points thus subjected to the reverse slip regime will come to be subjected to forward slip again, as expected owing to the remote loading. This means that any material point at the interface will be subjected over time to both reverse and forward slip. The physical implications of this finding are that the wear performance of an interface subjected to varying loads may be worse than expected if the interface's  $\chi$  parameter is sufficiently low – in practice, this reverse slip regime can be avoided if the friction coefficient is large, which paradoxically suggests that lubrication strategies relying on lowering the frictional coefficient to mitigate wear may in turn have a detrimental effect in the wear performance during transient loading. Owing to the potential relevance and specific loading conditions involved, this effect will be the subject of future in-depth work examining how non-linear frictional coefficients (e.g., velocity dependent frictional coefficients (Molinari and Perfettini, 2017; Perfettini and Molinari, 2017)), as well different loading regimes and contact geometries affect the existence of the reverse slip regime.

## 7. Conclusions

This article has focused on analysing the conditions of stick and slip under the transient elastodynamic contact of two elastically similar semi-infinite bodies loaded with sudden remote shock loads of constant magnitude in the normal and tangential directions. This loading launches interfacial normal and shear tractions, that propagate away from the edge of the contact zone at the longitudinal and transverse speeds of sound, respectively. As a result, the normal load that establishes the contact always precedes the tangential load. The *head wave* region influenced only by the normal load is a region of full stick, no shear tractions being present.

Depending on the loading conditions, it is possible that the imbalance between the applied interfacial tangential traction and the frictional forces may only be accommodated if the interface is allowed to slip. In such cases, we have offered a complete mathematical derivation of the elastodynamic 'corrective' traction acting at the interface. This corrective traction would allow for Coulomb's dry frictional law to be satisfied in the regions of interfacial slip. The corrective traction has been derived employing the Wiener-Hopf and Cagniard-de Hoop techniques. Albeit the approach is mathematically involved, the resulting expressions for the transformation kernels at the interface are relatively simple once they are regularised as proposed in this work.

The resulting mathematical expressions enable the extension of the classical Cattaneo-Mindlin problem to elastodynamics. However, owing to the inherent complexities of the formulation, the study of the stick and slip regions arising from the problem could only be approached numerically, for which a simple Nyström collocation method has been used.

The numerical solution has shown that the arrival at any point along the interface of the shear wave marks the onset of interfacial slip. This paper has argued that slip is necessary to accommodate the imbalance between shear and normal loads irrespective of the ratio between the remote tangential load,  $Q_0$ , and the frictional load  $fP_0$ . This is because away from the asymptotic near field at the edge of the contact interface, both loads follow distinct temporal evolutions that prevent fully stuck solutions from existing. However, for  $\chi = fP_0/Q_0 > 1$ , it is observed that the fully stuck solution is naturally achieved over time: the anomalous slip wave front that arises in this case tends to travel away from the edge of the contact zone, where conditions of full stick are achieved over time. Given the specific nature of the elastodynamic solutions, further investi-

gations are required as to the significance of this slip wave – and investigating the specific effects of the contact geometry will be the subject of future work. However, the anomalous slip wave is expected to be a source of vibrations and interfacial wear arising when the loading conditions at an interface are suddenly changed.

For conditions of partial slip, the elastodynamic contact problem reveals the existence of a transient regime of reverse slip if the tangential load is sufficiently large, or the friction coefficient sufficiently small. In either such case, the interfacial region between the shear wave and the Rayleigh wave will invariably be subjected to a regime of reverse slip that is later on restored to forward slip. Because this entails a change in the sign of the interfacial loads, it is expected that this transient would impact the wear performance of contact interfaces when present. Owing to the uncoupled nature of the problem, the imbalance between shear and normal loads cannot be accommodated through loss-of-contact. This does not prejudice the possibility of loss of contact if the normal load becomes tensile over a certain period of time, as could happen under purely harmonic vibrations.

Therefore, the findings of this article showcase the existence of a number of transient effects affecting contact interface that are missed in static treatments of the contact problem, but that as we have shown can now be captured explicitly and without recourse to stability analyses – in fact, many of these effects do not appear to entail an instability. The article provides a coherent mathematical formulation that enables the extension of most elastostatic contact problems of the Cattaneo-Mindlin type to time-dependent, fully transient situations. This formulation can be applied to study loading conditions different to those explored here. So long as the uncoupled assumption remains reasonable, it is possible to employ the same kernel functions and numerical approach to study mixed loading conditions, either between different dynamic loads (e.g. ramp or harmonic loading in the normal and/or shear loads), or between combinations of static and dynamic loading (e.g., constant normal loads but time-dependent shear loads, or viceversa). The effect of different geometries and of rarefaction waves incoming from free surfaces on the contact interface can also now be accounted for by simple superposition or convolution of the basic solutions reached in this article.

This study opens new lines of inquiry in a wide range of applications. On the one hand, the existence of temporally varying loads affecting the bearings of turbines, shafts or rotating machinery is well-known, and the proposed formulation enables the study the transients induced when loading and unloading said machinery. In such transients, this article has showed that interfacial vibrations are possible and an unavoidable feature of the transient, and that strategies relying on lowering friction via lubrication result in worse-than-expected wear performance. Equally so, contacting bodies subject to friction are a known feature of geophysical faults; in such cases, the formulation presented here offers a simple and exact way of tackling the modelling of seismological signals produced by said frictional faults.

## Acknowledgements

The author wishes to thank Prof D. Dini for his useful comments.

## Appendix A

The mathematical expression of  $\chi_R$  is the value (Eringen and Suhubi, 1975)

$$\chi_R = \frac{a^2(4b^2 - 6c^2) + 8k(\sqrt{a^2 - c^2}\sqrt{b^2 - c^2} + c^2) - 6b^2c^2}{\sqrt{a^2 - c^2}\sqrt{b^2 - c^2}} - 4b^2$$



where  $a = 1/c_l$ ,  $b = 1/c_t$ ,  $c = 1/c_R$ , and  $c_R$  is the Rayleigh wave speed, given by

$$c = -\frac{b^2(3b^2 - 2a^2)}{6(a^2 - b^2)} + \frac{\sqrt[3]{32a^6b^6 - 99a^4b^8 + 90a^2b^{10} + 3\sqrt{3}\sqrt{-64a^{10}b^{14} + 235a^8b^{16} - 340a^6b^{18} + 242a^4b^{20} - 84a^2b^{22} + 11b^{24} - 27b^{12}}}}{6 \cdot 2^{2/3}(a^2 - b^2)} - \frac{-256a^4b^4 + 384a^2b^6 - 192b^8}{192\sqrt[3]{2}(a^2 - b^2)\sqrt[3]{32a^6b^6 - 99a^4b^8 + 90a^2b^{10} + 3\sqrt{3}\sqrt{-64a^{10}b^{14} + 235a^8b^{16} - 340a^6b^{18} + 242a^4b^{20} - 84a^2b^{22} + 11b^{24} - 27b^{12}}}}$$

## Appendix B

We may rewrite the contact problem as

$$s_{II}(x, t) = -f \operatorname{sign}(f) p(x, t) - q(x, t) \equiv F(x, t)$$

where  $p(x, t)$  and  $q(x, t)$  are prescribed, and  $s_{II}(x, t)$  is regularised to

$$s_{II}(x, t) = \langle K_a, b_x \rangle + \langle K_b, b_x \rangle \quad (7.2)$$

In principle, the unknown is  $b_x(x, t)$  – the slip velocity density –, found as  $\langle b_x, K_a + K_b \rangle$ . The problem therefore can be thought of as a deconvolution problem, and is agreeable to a treatment similar to the antiplanar case given in Gurrutxaga-Lerma (2019).

However, for numerical regularity purposes, it becomes easier to use the coordinate transformation introduced in Section 4.4. In that event, we note that if  $x > 0$  and we set  $\tau/x = u'$ , we obtain:

$$p(x, t) \Rightarrow p(u) = -\frac{1}{\pi} \int_a^u \operatorname{Im}[\Sigma_+(-u')] du' H(u - a) \quad (7.3)$$

$$q(x, t) \Rightarrow q(u) = -\frac{1}{\pi} \int_a^u \operatorname{Im}[T_+(-u')] du' H(u - a) \quad (7.4)$$

The ensuing problem can then be solved as a 1D equation dependent on  $u$ , so that the  $x, t$  spatio-temporal variables may be reconstructed into  $(x, t)$  upon solution in  $u$ . Thus, we shall concern ourselves with the equation:

$$F(u) = s_{II}(u) = \langle K_a, B \rangle + \langle K_b, B \rangle \quad (7.5)$$

We shall solve this problem using a simple collocation method (Porter and Stirling, 1990; Atkinson, 1997) of the sort commonly employed to solve Volterra integral equations of the first kind (Martin and Rizzo, 1989; Vainikko, 1993). We thus define the discrete grid  $S_j = [u_j, u_{j+1}]$  and define some well-posed basis function set  $\{N_j(u)\}$  with compact support over  $[u_j, u_{j+1}]$  such that the velocity vector may be expressed as

$$B_x(u) = \sum_{i=0}^{n_u} \sum_{b=0}^{n_u} b_j N_j(u) \quad (7.6)$$

where  $b_j \in \mathbb{R}$  is a number, and  $n_u$  the total number of subintervals.

We insert Eq. (7.6) into the convolution integral to obtain

$$s_{II}(u) = \sum_j b_j \left[ \int_{\Gamma_a} N_i(u') K_a(u - u') du' + \int_{\Gamma_b} N_{ij}(u') K_b(u - u') du' \right] \quad (7.7)$$

We define a triangular basis function (Atkinson, 1997):

$$N_j^\Delta(u) = \begin{cases} \frac{u - u_{j-1}}{u_j - u_{j-1}} & u \in [u_{j-1}, u_j] \\ \frac{u_{j+1} - u}{u_{j+1} - u_j} & u \in [u_j, u_{j+1}] \\ 0 & \text{otherwise} \end{cases} \quad (7.8)$$

Crucially, with such simple form it is possible to perform an explicit integration of Eq. (7.7) with Eq. (7.8). A similar advantage to collocation methods in dynamic problems was observed by Martin and Rizzo (1989) and in Gurrutxaga-Lerma (2019), whereupon we reach an analytic form for the convolution of the kernel with  $N_{ij}$ . By calling  $L_j = \langle N_j^\Delta, K_a \rangle + \langle N_j^\Delta, K_b \rangle = L_j^{(a)} + L_j^{(b)}$ , we find

$$L_j^{(a)}(u) = \frac{4}{3} (u^2 - a^2)^{3/2} \quad (7.9)$$

$$L_j^{(b)}(u) = \frac{4}{3} \frac{(b^2 - u^2)^2}{\sqrt{u^2 - b^2}} + \arctan\left(\frac{\sqrt{u^2 - b^2}}{b}\right) \quad (7.10)$$

Thus, we seek to solve

$$F(u) = \sum_j b_j (L_j^{(a)}(u) + L_j^{(b)}(u)) = \sum_j b_j L_j(u) \quad (7.11)$$

for which we collocate  $n_u$  collocation points  $u_k$  mid-interval, so that  $u_k = u_j + \Delta u_j/2$ , with  $\Delta u_j = u_{j+1} - u_j$ . The choice of the collocation points mid-interval is done by inspection, although it is noted that given the nature of the basis functions, any other point would render the results open to further numerical instabilities. In any event, this leads to a linear system of  $n_u$  equations with  $n_u$  unknowns (the  $b_j$  nodal values), which can be solved numerically using conventional linear algebra techniques (q.v. Wendland, 2017):

$$F_k = b_j L_{jk} \quad (7.12)$$

The slip condition that  $\operatorname{sign}(\dot{u}) \equiv \operatorname{sign}(\dot{u})$  is checked for each  $j$  and if, necessary, the sign is reversed. This provides a map of the forward and reverse slip regions in the contact interface, if any. The resulting numerical model is solved in the  $(u)$  space. The  $(x, t)$  results are then obtained by converting node by node the  $u$  coordinate back to  $t$  as  $t \rightarrow u \cdot x$ .

## References

- Achenbach, J. D., 1973. Wave Propagation in Elastic Solids. North-Holland New York.
- Achenbach, J.D., Epstein, H.I., 1967. Dynamic interaction of a layer and a half-space. J. Eng. Mech. 93 (5), 27–42.
- Adams, G.G., 1995. Self-excited oscillations of two elastic half-spaces sliding with a constant coefficient of friction. J. Appl. Mech. 62 (4), 867–872.
- Adams, G.G., 1998. Dynamic instabilities in the sliding of two layered elastic half-spaces. J. Tribol. 120 (2), 289–295.
- Aki, K., Richards, P.G., 2002. Quantitative Seismology, second ed. University Science Books, Sausalito, CA.
- Amontons, M., 1699. De la resistance causée dans les machines, tant par les frottemens des parties qui les composent, que par roideur des cordes qu'on y emploie, et la maniere de calculer l'un et l'autre. In: Guérin, H.L., Jacques, r. S. (Eds.), Memoirs de l'Academie Royale. Gabriel Martin, Jean Baptiste Coignard fils, Paris, pp. 206–222.
- Atkinson, K.E., 1997. The numerical solution of integral equations of the second kind. Cambridge Monographs on Applied and Computational Mathematics. Cambridge University Press, Cambridge, UK.
- Barber, J.R., 2018. Contact Mechanics. Springer, Cham, CH.
- Barquins, M., 1985. Sliding friction of rubber and Schallamach waves—a review. Mater. Sci. Eng. 73, 45–63.
- Bedding, R.J., Willis, J.R., 1973. The dynamic indentation of an elastic half-space. J. Elast. 3 (4), 289–309.
- Ben-David, O., Cohen, G., Fineberg, J., 2010. The dynamics of the onset of frictional slip. Science 330 (6001), 211–214.
- Ben-David, O., Fineberg, J., 2011. Static friction coefficient is not a material constant. Phys. Rev. Lett. 106 (25), 254301.
- Berger, E.J., Begley, M.R., Mahajani, M., 2000. Structural dynamic effects on interface response: formulation and simulation under partial slipping conditions. J. Appl. Mech. 67 (4), 785–792.
- Borodich, F.M., Gomatam, J., 1998. An exact solution for the first stage of frictional collision of a die and an elastic half-space. Quart. J. Mech. Appl. Math. 51 (4), 563–576.
- Broberg, K.B., 1999. Cracks and Fracture. Academic Press, London.
- Brock, L.M., 1976. Symmetrical frictionless indentation over a uniformly expanding contact region—I. Basic analysis. Int. J. Eng. Sci. 14 (2), 191–199.
- Brock, L.M., 1978. Frictionless indentation by an elastic punch: a dynamic hertzian contact problem. J. Elast. 8 (4), 381–392.
- Brock, L.M., 1979. Rapid interface flaw extension with friction—I. Basic analysis. Int. J. Eng. Sci. 17 (1), 49–58.

- Brock, L.M., 1981. Sliding and indentation by a rigid half-wedge with friction and displacement coupling effects. *Int. J. Eng. Sci.* 19 (1), 33–40.
- Brock, L.M., 1982. Dynamic solutions for the non-uniform motion of an edge dislocation. *Int. J. Eng. Sci.* 20 (1), 113–118.
- Brock, L.M., 1993. Exact transient results for pure and grazing indentation with friction. *J. Elast.* 33 (2), 119–143.
- Brock, L.M., 2002. Exact analysis of dynamic sliding indentation at any constant speed on an orthotropic or transversely isotropic half-space. *J. Appl. Mech.* 69 (3), 340–345.
- Brock, L.M., Georgiadis, H.G., 1994. Dynamic frictional indentation of an elastic half-plane by a rigid punch. *J. Elast.* 35 (1–3), 223–249.
- Butlin, T., Woodhouse, J., 2009. Sensitivity studies of friction-induced vibration. *Int. J. Veh. Des.* 51 (1–2), 238–257.
- Cagniard, L., 1939. *Réflexion et Réfraction des ondes Séismique Progressives*. Gauthiers-Villars, Paris.
- Cattaneo, C., 1938. Sul contatto di due corpi elastici: distribuzione locale degli sforzi. *Rc. Accad. Naz. Lincei* 27, 342–348, 434–436, 474–478.
- Colin, J., 2016. Dynamic instability of two elastic half-spaces sliding with a rate-and-state friction constitutive law. *J. Appl. Mech.* 83 (12), 121004.
- Comninou, M., Dundurs, J., 1977. Elastic interface waves involving separation. *J. Appl. Mech.* 44 (2), 222–226.
- De Hoop, A.T., 1960. A modification of Cagniard's method for solving seismic pulse problems. *Appl. Sci. Res.* B 8, 349–356.
- Dini, D., Hills, D.A., 2003. A method based on asymptotics for the refined solution of almost complete partial slip contact problems. *Eur. J. Mech.-A/Solids* 22 (6), 851–859.
- Dini, D., Hills, D.A., 2004. Bounded asymptotic solutions for incomplete contacts in partial slip. *Int. J. Solids Struct.* 41 (24–25), 7049–7062.
- Dini, D., Sackfield, A., Hills, D.A., 2005. Comprehensive bounded asymptotic solutions for incomplete contacts in partial slip. *J. Mech. Phys. Solids* 53 (2), 437–454.
- Duffour, P., Woodhouse, J., 2004. Instability of systems with a frictional point contact. Part 1: basic modelling. *J. Sound Vib.* 271 (1–2), 365–390.
- Duffour, P., Woodhouse, J., 2004. Instability of systems with a frictional point contact. Part 2: model extensions. *J. Sound Vib.* 271 (1–2), 391–410.
- Duffour, P., Woodhouse, J., 2007. Instability of systems with a frictional point contact. Part 3: experimental tests. *J. Sound Vib.* 304 (1–2), 186–200.
- Eringen, A.C., Suhubi, E.S., 1975. *Elastodynamics*, 2. Academic Press, New York.
- Evans, L.C., 2010. *Partial differential equations*. Graduate Studies in Mathematics, second ed. American Mathematical Society.
- Freund, L.B., 1998. *Dynamic Fracture Mechanics*. Cambridge Univ. Press, Cambridge, UK.
- Galín, L.A., 1961. *Contact Problems in the Theory of Elasticity* (Trans. H. Moss). Technical report. North Carolina State University, Raleigh School of Physical Sciences and Applied Mathematics.
- Gaul, L., Lenz, J., 1997. Nonlinear dynamics of structures assembled by bolted joints. *Acta Mech.* 125 (1–4), 169–181.
- Gaul, L., Nitsche, R., 2001. The role of friction in mechanical joints. *ASME Appl. Mech. Rev.* 54, 93–110.
- Georgiadis, H.G., Barber, J.R., 1993. On the super-rayleigh/subseismic elastodynamic indentation problem. *J. Elast.* 31 (3), 141–161.
- Georgiadis, H.G., Brock, L.M., Rigatos, A.P., 1995. Dynamic indentation of an elastic half-plane by a rigid wedge: frictional and tangential-displacement effects. *Int. J. Solids Struct.* 32 (23), 3435–3450.
- Georgiadis, H.G., Charalambakis, N., 1994. An analytical/numerical approach for cracked elastic strips under concentrated loads—transient response. *Int. J. Fract.* 65 (1), 49–61.
- Gurrutxaga-Lerma, B., 2018. Static and dynamic multipolar field expansions of defects in crystals: dislocations and cracks. *Int. J. Eng. Sci.* 128, 165–186.
- Gurrutxaga-Lerma, B., 2019. On the transient dynamic antiplane contact problem in the presence of dry friction and slip. *Int. J. Solids Struct.* 170, 142–156.
- Gurrutxaga-Lerma, B., Balint, D.S., Dini, D., Eakins, D.E., Sutton, A.P., 2013. A dynamic discrete dislocation plasticity method for the simulation of plastic relaxation under shock loading. *Proc. R. Soc. A* 469, 20130141.
- Gurrutxaga-Lerma, B., Balint, D.S., Dini, D., Sutton, A.P., 2015. Elastodynamic image forces on dislocations. *Proc. R. Soc. A* 471, 20150433.
- Hills, D.A., Kelly, P.A., Dai, D.N., Korsunsky, A.M., 1996. *Solution of crack problems: the distributed dislocation technique*. Solid Mechanics and its Applications, vol. 44. Kluwer Academic Publishers, Boston.
- Hills, D.A., Nowell, D., 1994. *Mechanics of fretting fatigue*. Solid Mechanics and its Applications, vol. 30. Kluwer Academic Publishers, Dordrecht, NL.
- Hills, D.A., Thaitirarat, A., Barber, J.R., Dini, D., 2012. Correlation of fretting fatigue experimental results using an asymptotic approach. *Int. J. Fatig.* 43, 62–75.
- Hirani, H., Athre, K., Biswas, S., 1999. Dynamic analysis of engine bearings. *Int. J. Rotat. Mach.* 5 (4), 283–293.
- Johnson, K.L., 1987. *Contact Mechanics*. Cambridge Univ. Press, Cambridge, UK.
- Khonsari, M.M., Booser, E.R., 2008. *Applied Tribology: Bearing Design and Lubrication*, 12. John Wiley & Sons.
- Kostrov, B.V., 1964. Self-similar dynamic problems of the impression of a rigid die in an elastic half-space. *Izv. Akad. Nauk SSSR Mekh. Mashinostr.* 4, 54–62.
- Kotzalas, M.N., Doll, G.L., 2010. Tribological advancements for reliable wind turbine performance. *Philos. Trans. R. Soc. A* 368 (1929), 4829–4850.
- Kubenko, V.D., Popov, S.N., 1988. Two-dimensional problem of the impact of a rigid blunt body onto the surface of an elastic halfspace. *Int. Appl. Mech.* 24 (7), 693–700.
- Lamb, H., 1904. I. on the propagation of tremors over the surface of an elastic solid. *Philos. Trans. R. Soc. Lon. Ser. A* 203 (359–371), 1–42.
- Markushevich, A.I., 2005. *Theory of Functions of a Complex Variable*, vol. III, second ed. American Mathematical Society, Providence, RI.
- Martin, P.A., Rizzo, F.J., 1989. On boundary integral equations for crack problems. *Proc. R. Soc. Lond. A* 421, 341–355.
- Martins, J.A.C., Guimaraes, J., Faria, L.O., 1995. Dynamic surface solutions in linear elasticity and viscoelasticity with frictional boundary conditions. *J. Vibr. Acoust.* 117, 445–451.
- Menq, C.-H., Griffin, J.H., 1985. A comparison of transient and steady state finite element analyses of the forced response of a frictionally damped beam. *J. Vibr. Acoust.* 107 (1), 19–25.
- Miklowitz, J., 1978. *The Theory of Elastic Waves and Waveguides*. North-Holland.
- Mindlin, R.D., 1949. Compliance of elastic bodies in contact. *J. Appl. Mech.* 16, 259–268.
- Molinari, A., Perfettini, H., 2017. A micromechanical model of rate and state friction: 2. Effect of shear and normal stress changes. *J. Geophys. Res.* 122 (4), 2638–2652.
- Morren, J., Pierik, J., De Haan, S.W.H., 2006. Inertial response of variable speed wind turbines. *Electric Power Syst. Res.* 76 (11), 980–987.
- Nack, W.V., 2000. Brake squeal analysis by finite elements. *Int. J. Veh. Des.* 23 (3–4), 263–275.
- Noble, B., 1958. Methods based on the Wiener-Hopf technique for the solution of partial differential equations. *International Series of Monographs on Pure and Applied Mathematics*, vol. 7. Pergamon Press, New York.
- Nowell, D., Hills, D.A., Sackfield, A., 1988. Contact of dissimilar elastic cylinders under normal and tangential loading. *J. Mech. Phys. Solids* 36 (1), 59–75.
- Palm, E.C., Murphy, T.P., 1999. Very low friction rotator for use at low temperatures and high magnetic fields. *Rev. Sci. Instrum.* 70 (1), 237–239.
- Perfettini, H., Molinari, A., 2017. A micromechanical model of rate and state friction: 1. Static and dynamic sliding. *J. Geophys. Res.* 122 (4), 2590–2637.
- Persson, B.N.J., 2001. Elastic instabilities at a sliding interface. *Phys. Rev. B* 63 (10), 104101.
- Porter, D., Stirling, D.S.G., 1990. *Integral Equations*. Cambridge Univ. Press, Cambridge, UK.
- Renardy, M., 1992. Ill-posedness at the boundary for elastic solids sliding under coulomb friction. *J. Elast.* 27, 281–287.
- Robinson, A.R., Thompson, J.C., 1974. Transient stresses in an elastic half space resulting from the frictionless indentation of a rigid wedge-shaped die. *ZAMM* 54 (3), 139–144.
- Rubinstein, S.M., Cohen, G., Fineberg, J., 2004. Detachment fronts and the onset of dynamic friction. *Nature* 430 (7003), 1005.
- Rubinstein, S.M., Cohen, G., Fineberg, J., 2007. Dynamics of precursors to frictional sliding. *Phys. Rev. Lett.* 98 (22), 226103.
- Schallamach, A., 1971. How does rubber slide? *Wear* 17 (4), 301–312.
- Schwingshackl, C.W., Petrov, E.P., Ewins, D.J., 2012. Effects of contact interface parameters on vibration of turbine bladed disks with underplatform dampers. *J. Eng. Gas Turb. Power* 134 (3), 32507.
- Slepyan, L.I., Brun, M., 2012. Driving forces in moving-contact problems of dynamic elasticity: indentation, wedging and free sliding. *J. Mech. Phys. Solids* 60 (11), 1883–1906.
- Torkhani, M., May, L., Voinis, P., 2012. Light, medium and heavy partial rubs during speed transients of rotating machines: numerical simulation and experimental observation. *Mech. Syst. Signal Process.* 29, 45–66.
- Vainikko, G., 1993. *Multidimensional Weakly Singular Integral Equations*. Springer, Berlin.
- Weertman, J., 1980. Unstable slippage across a fault that separates elastic media of different elastic constants. *J. Geophys. Res.* 85 (B3), 1455–1461.
- Wendland, H., 2017. *Numerical Linear Algebra: An Introduction*, 56. Cambridge University Press, Cambridge, UK.
- Wiener, N., 1988. *The Fourier Integral and Certain of its Applications*. Cambridge Univ. Press, Cambridge, UK.
- Williams, J.A., 2001. Friction and wear of rotating pivots in MEMS and other small scale devices. *Wear* 251 (1–12), 965–972.